Biogeosciences
Open Access
Discussions

Nitrogen cycling in the subsurface biosphere: nitrate isotopes in porewaters underlying the oligotrophic North Atlantic

S. D. Wankel[1]**, C. Buchwald**[1]**, W. Ziebis**[2]**, C. B. Wenk**[3,a]**, and M. F. Lehmann**[3]

[1]Woods Hole Oceanographic Institution, Department of Marine Chemistry and Geochemistry, 266 Woods Hole Rd., Woods Hole, MA, 02543, USA
[2]University of Southern California, Department of Biological Sciences, Allan Hancock Foundation Building, Los Angeles, California, 90089, USA
[3]University of Basel, Department of Environmental Science, Bernoullistrasse 32, Basel, 4056, Switzerland
[a]now at: Weizmann Institute of Science, Department of Earth and Planetary Sciences, Rehovot, 7610001, Israel

BGD

12, 13545–13591, 2015

Nitrogen cycling in deep-sea porewaters

S. D. Wankel et al.

Title Page

Abstract	Introduction
Conclusions	References
Tables	Figures

|◀ | ▶|
◀ | ▶

Back | Close

Full Screen / Esc

Printer-friendly Version

Interactive Discussion

Abstract

Nitrogen (N) is a key component of fundamental biomolecules. Hence, the cycling and availability of N is a central factor governing the extent of ecosystems across the Earth. In the organic-lean sediment porewaters underlying the oligotrophic ocean, where low levels of microbial activity persist despite limited organic matter delivery from overlying water, the extent and modes of nitrogen transformations have not been widely investigated. Here we use the N and oxygen (O) isotopic composition of porewater nitrate (NO_3^-) from a site in the oligotrophic North Atlantic (IODP) to determine the extent and magnitude of microbial nitrate production (via nitrification) and consumption (via denitrification). We find that NO_3^- accumulates far above bottom seawater concentrations ($\sim 21\,\mu M$) throughout the sediment column (up to $\sim 50\,\mu M$) down to the oceanic basement as deep as 90 mbsf, reflecting the predominance of aerobic nitrification/remineralization within the deep marine sediments. Large changes in the $\delta^{15}N$ and $\delta^{18}O$ of nitrate, however, reveal variable influence of nitrate respiration across the three sites. We use an inverse porewater diffusion–reaction model, constrained by the N and O isotope systematics of nitrification and denitrification and the porewater NO_3^- isotopic composition, to estimate rates of nitrification and denitrification throughout the sediment column. Results indicate variability of reaction rates across and within the three boreholes that are generally consistent with the differential distribution of dissolved oxygen at this site, though not necessarily with the canonical view of how redox thresholds separate nitrate regeneration from dissimilative consumption spatially. That is, we provide isotope evidence for expanded zones of co-ocurring nitrification and denitrification. The isotope biogeochemical modeling also yielded estimates for the $\delta^{15}N$ and $\delta^{18}O$ of newly produced nitrate ($\delta^{15}N_{NTR}$ and $\delta^{18}O_{NTR}$), as well as the isotope effect for denitrification ($^{15}\varepsilon_{DNF}$), parameters with high relevance to global ocean models of N cycling. Estimated values of $\delta^{15}N_{NTR}$ were generally lower than previously reported $\delta^{15}N$ values for sinking PON in this region. We suggest that these values can be related to sedimentary N-fixation and remineralization of the newly fixed organic N.

Values of $\delta^{18}O_{NTR}$ generally ranged between −2.8 and 0.0‰, consistent with recent estimates based on lab cultures of nitrifying bacteria. Notably, some $\delta^{18}O_{NTR}$ values were elevated, suggesting incorporation of ^{18}O-enriched dissolved oxygen during nitrification, and possibly indicating a tight coupling of NH_4^+ and NO_2^- oxidation in this metabolically sluggish environment. Our findings indicate that the production of organic matter by in situ autotrophy (e.g., nitrification, nitrogen fixation) supply a large fraction of the biomass and organic substrate for heterotrophy in these sediments, supplementing the small organic matter pool derived from the overlying euphotic zone. This work sheds new light on an active nitrogen cycle operating, despite exceedingly low carbon inputs, in the deep sedimentary biosphere.

1 Introduction

Below the euphotic zone at the ocean surface, the dark ocean, including environments above and below the seafloor, hosts the largest habitable environment on the planet and is home to a wide range of globally relevant biogeochemical processes (Orcutt et al., 2011). While significant progress has been made in recent years toward characterizing the geological, chemical, and ecological composition of a variety of subsurface environments (Orcutt et al., 2011; Edwards et al., 2011, 2012b), the potential for impact of these systems on global biogeochemical cycles remains poorly understood. Most of our knowledge about subseafloor microbial activity stems from research focusing on productive continental margins, where relatively high fluxes of organic matter from surface primary productivity support a large heterotrophic and mostly anaerobic microbial community, (e.g., Blair and Aller, 2012). By comparison, vast areas of the seafloor, in particular those underlying ocean gyres, characterized by low primary productivity and low organic matter flux to the sea floor, have received far less attention (D'Hondt et al., 2009; Mason et al., 2010; Fischer et al., 2009). In contrast to well-studied ocean margin sediments, oxygen (O_2) and nitrate (NO_3^-), two powerful ox-

idants of organic carbon, penetrate deeply into the sediment underlying oligotrophic ocean waters (D'Hondt et al., 2009; Murray and Grundmanis, 1980; Rutgers van der Loeff et al., 1990; Sachs et al., 2009; D'Hondt et al., 2015; Røy et al., 2012; Fischer et al., 2009). Furthermore, where underlain by relatively young and permeably ocean

5 crust, O_2 and NO_3^- are also supplied via upward diffusion from oxic and nitrate-replete fluids flowing through basaltic basement as has been shown for the North Pond site, which is located on the western flank of the Mid-Atlantic Ridge (Orcutt et al., 2013; Ziebis et al., 2012). At North Pond, where the sediment cover is thin ($< \sim 25\,m$), O_2 penetrates the entire sediment column; where sediment thickness is elevated, condi-

10 tions become anoxic at mid-depths. Aerobic heterotrophic respiration likely dominates organic carbon oxidation in the upper sediment column. However, as organic carbon becomes limiting at greater depths, autotrophic processes (e.g., nitrification) are likely to gain relative importance. Further, there is evidence that the upward supply of oxidants from the basaltic basement supports increased microbial activity (Picard and

15 Ferdelman, 2011). However, a fundamental understanding of the relative importance of specific metabolic activities that drive and sustain subsurface communities is lacking. Because central ocean gyres cover roughly half of the global seafloor, understanding the nature of the biosphere hosted within these sediments may reveal important insights into its role in ocean scale dynamics of ocean nitrogen and carbon cycling. Here

20 we focus specifically on elucidating subsurface nitrogen cycling and its role in supporting heterotrophic and autotrophic processes in oligotrophic deep-ocean sediments underlying the North Atlantic Gyre, at North Pond (22°45′ N, 46°05′ W).

IODP Expedition 336 (Mid-Atlantic Ridge Microbiology, 16 September–16 November 2011) aimed to directly address the nature of microbial communities in both ocean

25 crust and sediments at North Pond, a characteristic sediment-filled 70 km² depression surrounded by high relief topography common to the western flank of the Mid-Atlantic Ridge (Becker et al., 2001; Langseth et al., 1992). While a majority of seafloor subsurface biosphere research has focused on aspects of sediment carbon, sulfur and iron cycles, the potential role of N in supporting subsurface microbial activity has been

largely unexplored. Despite exceedingly oligotrophic conditions, life persists and evidence for active heterotrophic and autotrophic microbial communities in North Pond sediments is mounting (Ziebis et al., 2012; Picard and Ferdelman, 2011; Orcutt et al., 2013).

Nitrogen plays a central role as a limiting nutrient in many regions of the sunlit surface ocean (Rabalais, 2002), as nearly 90 % of the biologically available fixed N in the ocean resides below the euphotic zone in the deep ocean NO_3^- reservoir (Gruber, 2008). Globally, sediments (especially continental shelves) are considered a net sink of fixed nitrogen through reductive anaerobic processes including denitrification and anaerobic ammonium oxidation (Christensen et al., 1987; Devol, 1991; Prokopenko et al., 2013). However, there is abundant evidence demonstrating the importance of both oxidative and reductive N cycling processes (and their tight coupling) operating in sediment environments. For example, coupled nitrification (the chemolithotrophic oxidation of NH_4^+ to NO_3^-) and denitrification (the generally heterotrophic reduction of NO_3^- to N_2) have been shown be important in N budgets in sediments of continental shelves/margins and estuaries (Risgaard-Petersen, 2003; Granger et al., 2011; Lehmann et al., 2004, 2005; Wankel et al., 2009). In contrast to sediments on continental shelves, however, data from sediments underlying large swaths of the oligotrophic ocean suggest an entirely different framework. For example, NO_3^- concentration data from North Pond demonstrate an accumulation of NO_3^- with depth (Ziebis et al., 2012) implicating the role of in situ productivity supported by the autotrophic oxidation of ammonium and nitrite (e.g., nitrification). To what degree this NO_3^- pool supports other subsurface microbial communities as an electron acceptor, however, remains unclear. In addition, the supply of dissolved substrates (O_2, NO_3^-, DOC) from the underlying crustal aquifer may play a primary role in supporting these deep sediment communities. This geochemical exchange among crust, ocean and sediments across vast reaches of the seafloor, and its link to subsurface microbial activity, underscores its potential importance in global biogeochemical cycles.

Dual isotopes of NO_3^- represent a powerful tool for disentangling the combined activities of multiple N cycling processes (Casciotti et al., 2008; Lehmann et al., 2005; Sigman et al., 2005; Wankel et al., 2007; Marconi et al., 2015; Fawcett et al., 2015). Nitrate-removal processes (whether assimilatory or dissimilatory) have been shown to impart tightly coupled increases in both N and O isotope ratios of the remaining NO_3^- pool (Karsh et al., 2012; Kritee et al., 2012; Granger et al., 2008, 2004). In contrast, however, nitrification, the two-step oxidation of NH_4^+ to NO_2^- followed by NO_2^- oxidation to NO_3^-, represents a decoupling of the N and O isotope systems for nitrate (Casciotti and McIlvin, 2007; Buchwald and Casciotti, 2013; Wankel et al., 2007). Whereas the N atoms derive from the NH_4^+ (which can be assumed to derive from the sedimentary organic nitrogen pool), the oxygen atoms derive, to varying degrees, from both water and dissolved O_2 (Buchwald and Casciotti, 2010; Buchwald et al., 2012; Casciotti et al., 2010). Thus, by combining isotope mass balances of both N and O in the NO_3^- system, along with our understanding of organism-level constraints on the isotope systematics of these transformations, we can deduce the relative roles of multiple N cycling processes (e.g., Wankel et al., 2009; Lehmann et al., 2004; Bourbonnais et al., 2009). Here we use the dual isotopic composition of nitrate (N and O isotopes) as a record of microbial processes occurring in the low-energy sediments of North Pond underlying the oligotrophic North Atlantic gyre. By combining the N and O isotope mass balance constraints with an inverse reaction-diffusion model approach, we use these data to estimate rates of nitrification and denitrification, and to provide new constraints on some isotope parameters for these processes.

2 Material and methods

2.1 Sediment and porewater collection

Sediment cores were collected at three sites in the North Pond Basin as part of the IODP Leg 336 expedition and have been described extensively elsewhere (Expedition-

Full Screen / Esc

Printer-friendly Version

Interactive Discussion

336-Scientists, 2012a). Four boreholes were drilled (U1382B, U1383D, U1383E and U1384A, referred to hereafter as "2B", "3D", "3E" and "4A"). Sites 3D and 3E were next to each other and as drilling logs indicated that the core from 3E showed excessive signs of disturbance upon retrieval and potential contamination by seawater, it was not
5 used further in this project. Sediment cores were retrieved using the Advanced Piston Corer, which penetrated the seafloor sediments until contact with basement, followed by extended core barrel coring of the upper section of basement rock. Site 2B (~ 90 m sediment thickness, depth to basement) is located in the deeper part of the pond, approximately 25 m away from DSDP "legacy hole" 395A, which was instrumented as
10 CORK observatory (Davis et al., 1992). Site 3D (~ 42 m sediment thickness, depth to basement) lies in the northeastern region towards the edge of North Pond (~ 5.9 km away from U1382A), whereas site 4A (~ 95 m sediment thickness, depth to basement) is located on the northwest side in a deeper part of the basin, approximately 3.9 and 6.2 km distance from U1383 and U1382, respectively. All sediments were comprised
15 of light-brown to brown nannofossil ooze with intercalations of foraminiferal sand. In the lowest few meters close to the sediment/basement contact, sediments exhibited a darker brown color and sometimes rust-colored clay-rich zones (Edwards et al., 2012a; Expedition-336-Scientists, 2012b).

Porewater samples for concentration and stable isotope analyses were collected ei-
20 ther directly from cores on the shipboard catwalk during core retrieval (using methods described elsewhere Expedition-336-Scientists, 2012a) or from whole core rounds (~ 10 cm core sections) that were preserved at $-80\,^{\circ}$C. Whole core rounds were transported frozen and thawed only during lab-based porewater extraction. Porewaters were extracted on the ship and in the lab using rhizon samplers (0.2 µm) (Seeberg-Elverfeldt
25 et al., 2005). Approximately 40 mL of porewater was extracted from each 10 cm whole core round.

2.2 Nitrate concentrations

Porewaters for nitrate samples were collected from three sources: (1) shipboard pore-water extraction directly after core retrieval, (2) laboratory porewater extraction via rhizons from whole core rounds which had been frozen at −80 °C for ∼ 1 year after retrieval and (3) laboratory porewater extractions of subsampled sediments collected shipboard and stored at −20 °C for ∼ 9 months. Concentrations of NO_3^- (plus NO_2^-) from group 1 were measured via ion chromatography ∼ 3 months after collection, while concentrations from groups 2 and 3 were measured by chemiluminescence after reduction in a hot acidic vanadyl sulfate solution on a NO_x analyzer (Braman and Hendrix, 1989). Concentrations of NO_2^- were quantified by using the Griess-Ilosvay method followed by measuring absorption 540 nm or by chemiluminescence in a sodium iodide solution on a NO_x analyzer (Braman and Hendrix, 1989), and NO_3^- was quantified by difference (Grasshoff et al., 2007).

2.3 Nitrate stable isotope composition

Nitrate N and O isotopic composition were measured using the denitrifier method (Casciotti et al., 2002; Sigman et al., 2001), in which sample NO_3^- is quantitatively converted to N_2O using a lab-grown denitrifying bacterium before being extracted and purified on a purge and trap system similar to that previously described (McIlvin and Casciotti, 2010). Where detected, NO_2^- was removed by sulfamic acid addition (Granger and Sigman, 2009) prior to isotopic analysis of NO_3^-. Isotope ratios were measured on an IsoPrime100 (Elementar, Inc.) and corrections for drift, size and fractionation of O isotopes during bacterial conversion were carried out as previously described using NO_3^- standards USGS 32, USGS 34 and USGS 35 (Casciotti et al., 2002; McIlvin and Casciotti, 2011), with a typical reproducibility of 0.2 and 0.4 ‰ for $\delta^{15}N$ and $\delta^{18}O$, respectively.

3 Results

3.1 Dissolved oxygen profiles

Oxygen penetration depths, which have been discussed previously (Orcutt et al., 2013), vary distinctly among the three sites at North Pond indicating much greater respiratory consumption in 2B than in the profiles of other two sites, 3D and 4A (Fig. 1). In 2B, dissolved oxygen levels are drawn down to near detection by a depth of about 10 m (although low levels of dissolved O_2 seem to persist as deep as 30 m). In contrast, at site 3D, dissolved O_2 levels are drawn down to detection level for an interval of only ~ 3 m between a depth of ~ 30 to ~ 33 m and in 4A, zero-level O_2 concentrations were observed over the interval between 32 and 54 m. At North Pond, O_2 (and NO_3^-) is also supplied via diffusion from the underlying basaltic crustal aquifer (Fig. 1) (Orcutt et al., 2013; Ziebis et al., 2012).

3.2 NO_3^- and NO_2^- concentration profiles

Bottom seawater NO_3^- concentration at North Pond is approximately 21.6 µM (Ziebis et al., 2012). At all depths in all three profiles, porewater NO_3^- concentrations exceeded bottom water NO_3^- concentrations, reflecting the production of NO_3^- by nitrification and the net flux of NO_3^- to the overlying water from this site of ~ 4.6 µmoles m^{-2} d^{-1} (Ziebis et al., 2012), consistent with other studies of NO_3^- fluxes in pelagic deep-sea sediments (Berelson et al., 1990; Goloway and Bender, 1982; Hammond et al., 1996; Jahnke et al., 1982; Grundmanis and Murray, 1982). More precisely, below the sediment–water interface, NO_3^- concentrations increased significantly with depth (Fig. 1), before decreasing again with proximity to the basement/sediment contact. Mid-profile NO_3^- concentration maxima reached 38.2, 42.2 and 49.1 µM at depths of 19.1, 23.0 and 56.3 mbsf in the cores from sites 2B, 3D and 4A, respectively, – depths that generally coincided with O_2 concentrations below 10 µM. Nitrite was below detection at sites 3D

and 4A and was only detected at anoxic depths in site 2B (Fig. 1), where concentrations of up to 6.0 and 6.6 µM were observed at depths of 36 and 59 m, respectively.

3.3 NO_3^- N and O isotopic composition

Down-core changes in δ^{15}N and δ^{18}O varied markedly among the three cores (Fig. 1). The most prominent changes in both δ^{15}N and δ^{18}O were observed at site 2B (which had the most extensive O_2 deficient zone), in which δ^{15}N increased with depth from a value of +5.4‰ (bottom seawater) to a maximum of +23.3‰ at a depth of 59.2 mbsf and δ^{18}O increased from a bottom seawater value of +1.8‰ to a maximum of +23.8‰ at a much shallower depth of 32.1 mbsf. Isotopic maxima generally coincided with depths of lowest O_2 concentrations, except in 3D where the maxima fell slightly deeper than the O_2 minimum (Fig. 1). Substantial N and O isotopic shifts were also observed site 3D, in which increases above bottom water NO_3^- values to δ^{15}N of +11.8‰ and a δ^{18}O of +21.7‰ were observed, with both maxima occurring at a depth of 37 mbsf. In contrast, site 4A exhibited only very modest changes relative to bottom seawater, with a maximum δ^{15}N value of +7.0‰ at a depth of 38.8 mbsf and a maximum δ^{18}O value of +6.3‰ at a depth of 44.1 mbsf. Strong correlations were also observed between $\delta^{15}N_{NO_3}$ and $\delta^{18}O_{NO_3}$ (Fig. 2), with $\delta^{18}O_{NO_3}$ values always increasing more than the corresponding $\delta^{15}N_{NO_3^-}$. The relationship between $\delta^{18}O_{NO_3}$ and $\delta^{15}N_{NO_3}$ exhibited a slope of 1.8 for the upper portion of the 2B profile, 3.0 for the 3D profile and 2.4 for the 4A profile – consistently exceeding the 1 : 1 relationship expected from NO_3^- consumption alone. In 2B, sampling points near the most O_2 depleted depths and the lower portion of the profile fell closer to the expected 1 : 1 line for NO_3^- consumption by denitrification (Fig. 2).

4 Discussion

The distribution of porewater nitrate in deep-sea sediments is controlled by the combined influence of diffusion as well as several biologically catalyzed diagenetic processes including nitrification (ammonia and nitrite oxidation to nitrate) and denitrification (loss of N via nitrate reduction to gas phase products, NO, N_2O or N_2). Here we use the concentration and dual N and O stable isotope composition of porewater NO_3^- to gain insight into the magnitude and distribution of N transformation processes. In comparison to models that predict the rates of these processes based solely on concentration profiles of NO_3^- and O_2, for example, our approach estimates rates using the added constraints provided by recent studies of N and O isotope systematics of nitrification and denitrification (Granger et al., 2008; Buchwald and Casciotti, 2010; Casciotti et al., 2010; Buchwald et al., 2012). In particular, while there are strong and related N and O isotope effects during denitrification (Granger et al., 2008), the N and O source atoms during nitrate production are unrelated (Buchwald and Casciotti, 2010; Casciotti et al., 2010; Buchwald et al., 2012). Thus, changes in N and O isotopic composition between intervals of any one depth are the combined result of both diffusion of NO_3^- to/from overlying (and underlying) seawater, together with microbially mediated production and/or consumption of NO_3^- within porewaters. Under low oxygen, NO_3^- respiration by denitrification leads to a well-characterized increase in both $\delta^{15}N$ and $\delta^{18}O$ in conjunction with decreasing NO_3^- concentrations. In contrast, nitrification produces NO_3^- with a $\delta^{15}N$ equal to the starting NH_4^+ (when accumulation of NH_4^+ and NO_2^- is negligible), while the $\delta^{18}O$ of the newly produced NO_3^- is related to the $\delta^{18}O$ of ambient H_2O and O_2, as well as kinetic and equilibrium isotope effects associated with the stepwise oxidation of NH_4^+ to NO_3^-. While elevated NO_3^- concentrations indicate nitrification, extensive zones of low O_2 (and NO_3^- replete) porewaters also suggest a high potential for denitrification, which can be verified using nitrate dual isotope measurements. In this way, our modeling approach provides an assessment of the distribution of these N transformations, as well as some additional insights on the nature of N and

O source atoms to NO_3^- in these energy-lean systems. Specifically, we show below that the profiles of $\delta^{15}N_{NO_3}$ and $\delta^{18}O_{NO_3}$ can be explained by variations in the magnitude of nitrification and denitrification occurring throughout the sediment column, including substantial zones of overlap of these canonically aerobic/anaerobic processes. Finally, we use our model to predict the $\delta^{18}O$ and $\delta^{15}N$ stemming from nitrate production by nitrification, offering insights into both the nature of processes setting the O isotopic composition of oceanic NO_3^-, as well as the sources of N and/or the isotopic partitioning of available N sources in global ocean sediments.

4.1 Diffusion–reaction model

The diffusion–reaction inverse modeling approach used here is conceptually similar to other early diagenetic models that simulate porewater profiles of dissolved species through a sediment column harboring both oxic and anoxic organic matter remineralization (Christensen and Rowe, 1984; Goloway and Bender, 1982; Jahnke et al., 1982). It is an inverse modeling approach adapted to distinguish between heavy and light nitrate isotopologues (e.g., Lehmann et al., 2007). Specifically, we use the model to estimate rates of nitrification and denitrification required to fit the concentration profiles of each isotopologue, $^{14}NO_3^-$, $^{15}NO_3^-$, $N^{16}O_3^-$, and $N^{18}O_3^-$ (and, thus, $\delta^{15}N_{NO_3}$ and $\delta^{18}O_{NO_3}$ values) under the assumption of steady-state diffusion and microbial production (by nitrification) and/or consumption (by denitrification). Rates of nitrification and denitrification in each porewater sampling interval (e.g., defined as the distance between the lower and upper midpoints between sampling depths) were estimated numerically by least squares fitting of the system of equations describing the distribution of each isotopologue (using a genetic algorithm included in the Solver package of Microsoft Excel 2011). This approach involves determination of a non-unique solution using numerical iteration and optimization, and is repeatedly iterated to evaluate robustness of model fits. Certain parameters are allowed to be optimizable by the model, including both the magnitude of, and connection between, the N and O isotope effects for denitrification

($^{15}\varepsilon_{DNF}$ and $^{18}\varepsilon_{DNF}$:$^{15}\varepsilon_{DNF}$, respectively), as well as the N and O isotopic composition of new NO_3^- produced by nitrification ($\delta^{15}N_{NTR}$ and $\delta^{18}O_{NTR}$, respectively). Uncertainty in model-estimates is expressed as the standard error of 10 model-run estimates (Table 1). Conditions at the uppermost part of the sediment column were constrained

5 by measured concentrations and isotope ratios in bottom seawater. Measured concentrations of the NO_3^- isotopologues within each interval, together with the diffusive fluxes defined by the concentration gradients between the over/underlying intervals, were used for model fitting by least-squares optimization of microbial rates of nitrification and/or denitrification.

10 As measurable NH_4^+ was not observed at any depths, it is not modeled as such. NO_3^- is the only dissolved N species included in the model and we assume that all NH_4^+ generated by remineralization is completely oxidized to NO_3^- (see below). To minimize complexity, other diagenetic reactions that may be important in many sedimentary environments, including anaerobic NH_4^+ oxidation, removal of N species through inter-

15 actions with Fe or Mn and the adsorption and retention of NH_4^+ by clay minerals are not specifically addressed. We also neglect effects of compaction as well as potential changes in organic matter reactivity with depth. No difference in the diffusivity among NO_3^- isotopologues was included, since these differences are considered to be very small (Clark and Fritz, 1997).

20 Resolving the vertical dimension only, the mass balance differential equations are as follows:

$$\frac{\partial C_{14_{NO_3}}}{\partial t} = \frac{\partial}{\partial z}\left(D_{NO_3}\frac{\partial C_{14_{NO_3}}}{\partial z}\right) - DNF_{14_N} + NTR_{14_N} \tag{1}$$

$$\frac{\partial C_{15_{NO_3}}}{\partial t} = \frac{\partial}{\partial z}\left(D_{NO_3}\frac{\partial C_{15_{NO_3}}}{\partial z}\right) - DNF_{15_N} + NTR_{15_N} \tag{2}$$

$$\frac{\partial C_{16_{NO_3}}}{\partial t} = \frac{\partial}{\partial z}\left(D_{NO_3}\frac{\partial C_{16_{NO_3}}}{\partial z}\right) - DNF_{16_O} + NTR_{16_O} \tag{3}$$

Printer-friendly Version

Interactive Discussion

$$\frac{\partial C_{18_{NO_3}}}{\partial t} = \frac{\partial}{\partial z}\left(D_{NO_3}\frac{\partial C_{18_{NO_3}}}{\partial z}\right) - DNF_{18_O} + NTR_{18_O} \qquad (4)$$

such that for denitrification (DNF):

$$DNF_{14_N} = C_{14_{NO_3}} \times k_{DNF} \qquad (5a)$$

$$DNF_{15_N} = C_{15_{NO_3}} \times k_{DNF}/\alpha_{DNF} \qquad (5b)$$

$$DNF_{16_O} = C_{16_{NO_3}} \times k_{DNF} \qquad (5c)$$

$$DNF_{18_O} = C_{18_{NO_3}} \times k_{DNF}\Big/\left[1 + \left((\alpha_{DNF} - 1) \times \left(^{18}\varepsilon{:}^{15}\varepsilon_{DNF}\right)\right)\right] \qquad (5d)$$

$$DNF = DNF_{14_N} + DNF_{15_N} = DNF_{16_O} + DNF_{18_O} \qquad (6)$$

where D refers to the molecular diffusion coefficient for NO_3^- adjusted for porosity, DNF and NTR refers to the reaction rate of denitrification or nitrification, respectively (in mass volume^{-1} time^{-1}), C refers to the concentration of each isotopologue (in mass volume^{-1}) and k refers to the first order rate constant (time^{-1}). The fractionation factor, α, is defined as the ratio of rate constants for the light isotope over the heavy isotope (e.g., $^{15}\alpha = ^{14}k/^{15}k$) for a given process, alternatively expressed in terms of epsilon where $\varepsilon = (\alpha - 1) \times 1000$ in units of permil (‰). The term $^{18}\varepsilon{:}^{15}\varepsilon_{DNF}$ refers to the degree of coupling between the N and O isotope fractionation during denitrification, with a value of 1 indicating the two isotope effects are identical.

For the $\delta^{15}N$ and $\delta^{18}O$ of nitrification (NTR)

$$NTR_{14_N} = NTR \times f_{14_{NNTR}} \qquad (7a)$$

$$NTR_{15_N} = NTR \times f_{15_{NNTR}} \qquad (7b)$$

$$NTR_{16_O} = NTR \times f_{16_{ONTR}} \qquad (7c)$$

$$NTR_{18_O} = NTR \times f_{18_{ONTR}} \qquad (7d)$$

Full Screen / Esc

Printer-friendly Version

Interactive Discussion

where f refers to the fractional abundance of a particular isotopologue and

$$NTR = NTR_{^{14}N} + NTR_{^{15}N} = NTR_{^{16}O} + NTR_{^{18}O} \tag{8}$$

$$f_{^{14}NNTR} = 1/(1 + {}^{15}R_{NTR}) \tag{9a}$$

$$f_{^{15}NNTR} = 1 - f_{^{14}NNTR} \tag{9b}$$

$${}^{15}R_{NTR} = \left[{}^{15}N/{}^{14}N\right]_{NTR} \tag{9c}$$

and

$$f_{^{16}ONTR} = 1/(1 + {}^{18}R_{NTR}) \tag{10a}$$

$$f_{^{18}ONTR} = 1 - f_{^{16}ONTR} \tag{10b}$$

$${}^{18}R_{NTR} = \left[{}^{18}O/{}^{16}O\right]_{NTR} \tag{10c}$$

and ${}^{15}R_{NTR}$ and ${}^{18}R_{NTR}$ are used to calculate the $\delta^{15}N_{NTR}$ and $\delta^{18}O_{NTR}$, respectively.

For parameterizing diffusion, we use a porewater diffusion coefficient (D_s) based on the molecular diffusion coefficient (D_m at 5 °C) for NO_3^- of 1.05×10^{-5} cm^2 s^{-1} (Li and Gregory, 1974) adjusted for an average porosity (φ) of North Pond sediments of 64 % (Expedition-336-Scientists, 2012a), where $D_s = \varphi^k D_m$ and k is an empirically derived factor (we use 2.6) accounting for tortuosity of pore space (Hammond et al., 1996; McManus et al., 1995).

Compared with contemporaneous profiles of O_2 and Sr (Orcutt et al., 2013) and other dissolved ions, the NO_3^- concentration profiles suffer from some apparent analytical noise. The nature of the heterogeneity for NO_3^- concentration measurements was unclear. However, it is unlikely that this heterogeneity is environmental and we attribute it to small amounts of evaporation during freezer storage of the sediments, which is

supported by the apparent smoothness of the isotopic measurements (evaporation would change the apparent concentrations without influencing the isotopic composition of solutes such as NO_3^-). As such, for the purpose of the diffusion–reaction model, we applied a 5-point weighted triangular smoothing to the concentration data to eliminate outliers and unrealistically sharp gradients (Fig. 1). Given the relatively smooth and contiguous vertical profiles of $\delta^{15}N_{NO_3}$ and $\delta^{18}O_{NO_3}$, only very minor smoothing to these data was required using a similar approach (Fig. 1).

Within this model architecture, we explore the influence of four key parameters that could affect the estimation of nitrification and denitrification rates by this isotope mass balance approach, specifically, $^{15}\varepsilon_{DNF}$, $^{18}\varepsilon:^{15}\varepsilon_{DNF}$, $\delta^{15}N_{NTR}$ and $\delta^{18}O_{NTR}$. Specifically, the expression of the full enzymatic level isotope effect ($^{15}\varepsilon_{DNF}$) for denitrification (27‰) can be influenced by electron donor, carbon substrate quality, denitrification rate and metabolic activity (Kritee et al., 2012). Moreover, although the relationship between the kinetic isotope effects for ^{18}O and ^{15}N during respiratory consumption of NO_3^- by denitrification (e.g., $^{18}\varepsilon:^{15}\varepsilon_{DNF}$) has been shown to remain consistent at 1 : 1, the potential influence of nitrate reduction by periplasmic nitrate reductase (Nap), which imparts a lower $^{18}\varepsilon:^{15}\varepsilon_{DNF}$ value of 0.6 (Granger et al., 2008; Frey et al., 2014), could play a role in the dual isotope trajectory of NO_3^- consumption (Wenk et al., 2014). Further, in the absence of NH_4^+ accumulation in these sediments, the $\delta^{15}N_{NTR}$ is equal to the source of NH_4^+ being oxidized to NO_3^-, which is related to the $\delta^{15}N$ of the organic matter being remineralized. The $\delta^{18}O_{NTR}$ stems from a combination of factors including the $\delta^{18}O$ of the water and dissolved O_2 as well as the expression of kinetic isotope effects associated with the incorporation of O atoms from these pools (Buchwald and Casciotti, 2010; Casciotti et al., 2010; Andersson and Hooper, 1983). Below, we use the model to optimize and predict these values and to explore the sensitivity of rate estimates to $^{15}\varepsilon_{DNF}$.

The model contains more parameters than can be explicitly estimated from the small number of data points measured. To minimize the number of variables as much as

possible (and maximize the utility of the approach for constraining other variables), we adapt the model implementation for three different O_2 regimes: (1) "oxic intervals" where O_2 is poised as the more energy-yielding oxidant with respect to NO_3^- (here generally $O_2 > \sim 40\mu M$, see below) and in which only nitrification is allowed to occur,

5 (2) "transitional intervals" in which both denitrification and nitrification may occur (O_2 between ~ 40 and $2\mu M$) and (3) "anoxic intervals" where O_2 is $< 2\mu M$ and in which only denitrification is allowed to occur. In the oxic intervals – the model is used for parameter estimation of both $\delta^{15}N_{NTR}$ and $\delta^{18}O_{NTR}$ (in addition to nitrification rate), while in the anoxic intervals the model is used to estimate $^{15}\varepsilon_{DNF}$ and $^{18}\varepsilon:^{15}\varepsilon_{DNF}$ (in

10 addition to denitrification rate). In transitional intervals, $^{15}\varepsilon_{DNF}$ and $^{18}\varepsilon:^{15}\varepsilon_{DNF}$ are held constant at 25 ‰ and 1, respectively, and the parameter $\delta^{15}N_{NTR}$ and $\delta^{18}O_{NTR}$ are estimated through model fitting, together with rates of both nitrification and denitrification. In accordance with previous experimental work (Buchwald and Casciotti, 2010; Buchwald et al., 2012; Casciotti et al., 2010), the allowed range of values for $\delta^{15}N_{NTR}$ and

15 $\delta^{18}O_{NTR}$ were set to −5 to +10‰ and −5 to +20‰, respectively. When $^{15}\varepsilon_{DNF}$ and $^{18}\varepsilon:^{15}\varepsilon_{DNF}$ were estimated, values were restricted to within a range of 0 to 30‰ and 0.6 to 1.2, respectively.

4.2   Model results and implications

4.2.1   Model estimated rates of nitrification and denitrification

20 Profiles of sedimentary porewater solutes reflect the combined influence of many processes including diagenetic reactions, which are intimately related to the availability, abundance and quality of organic carbon. In particular, the distribution of dissolved substrates that are available as electron acceptors for microbial respiration of organic carbon, generally reflect stepwise consumption by the most thermodynamically (and

25 kinetically) favorable metabolic processes (e.g., O_2 consumption precedes NO_3^- consumption, which precedes sulfate reduction, etc.). While in organic rich estuarine and

continental shelf sediments, dissolved O_2 and NO_3^- are typically consumed within a few cm or mm below the sediment–seawater interface, sediments underlying large areas of the oligotrophic ocean are characterized by very deep penetration of O_2, in some cases even penetrating to the underlying ocean crust (D'Hondt et al., 2015, 2009; Orcutt et al., 2013; Ziebis et al., 2012). In connection with this deep penetration of O_2, deep-sea sediment porewaters also often exhibit extensive accumulation of NO_3^- above ambient seawater concentrations, associated with the oxidation of NH_4^+ released by aerobic remineralization of sediment organic matter (and linked to the consumption of O_2 through Redfield stoichiometry) (Berelson et al., 1990; Christensen and Rowe, 1984; D'Hondt et al., 2009; Goloway and Bender, 1982; Seitzinger et al., 1984). In organic-rich sediments, NO_3^- concentration profiles may exhibit maxima only a few mm or cm below the sediment/water interface. In contrast, in the deep-sea sediments underlying the oligotrophic regions of the ocean, the sedimentary zone where NO_3^- accumulates to 10 to 30 µM above bottom seawater concentrations can extend over a much larger vertical extent and nitrate maxima can be found tens of meters below the seafloor. In effect, the redox zonation of O_2 respiration, NH_4^+ oxidation, NO_2^- oxidation and NO_3^- reduction extends over larger depth ranges, and, depending on sediment thickness and organic carbon content – the redox state of these sediments may never reach the potential for NO_3^- reduction to play a role as a thermodynamically viable metabolic pathway.

While it is not necessarily apparent whether any NO_3^- respiration is occurring based on concentration profiles alone, dramatic increases in the $\delta^{15}N$ and $\delta^{18}O$ of NO_3^- with depth into the anoxic sediment intervals were observed in both 2B and 3D (Fig. 1) – indicating isotope fractionation by denitrification. The highest $\delta^{15}N$ and $\delta^{18}O$ values in 2B (+22.2 and +21.8‰, respectively) generally coincide with the lowest dissolved O_2, while highest $\delta^{15}N$ and $\delta^{18}O$ values in 3D (+11.8 and +19.7‰, respectively) fall just below the depth of lowest O_2. In stark contrast, 4A porewaters exhibit only a minor increase in $\delta^{18}O$ of $\sim 2.7‰$ within the anoxic interval, while $\delta^{15}N$ increased by only 0.8‰ (Fig. 1). The stark distinction between 2B/3D and 4A notwithstanding, the dual

isotopic composition and concentrations of NO_3^- in these porewaters reveals active nitrogen cycling processes within all three sites.

Using these changes in dual NO_3^- isotopic composition and concentration, we calculated the rates of nitrification and denitrification necessary to produce the observed patterns within each interval (in the transitional intervals, here we prescribe a value of 25‰ for $^{15}\varepsilon_{DNF}$, but explore the model sensitivity to this value later). Rates of nitrification and denitrification varied with depth, as well as across the three sites (Fig. 3; Table 1). Estimated rates of nitrification in the oxic and transitional intervals were up to 871 $nmol\,cm^{-3}\,yr^{-1}$, while rates of denitrification in the anoxic and transitional intervals reached up to 579 $nmol\,cm^{-3}\,yr^{-1}$ (Fig. 3; Table 1). By comparison, maximum rates of nitrification estimated from O_2 and NO_3^- profiles in the South Pacific Gyre, perhaps the most organic matter depleted seafloor sediments in the world, were predicted to be only as high as 18–74 $nmol\,cm^{-3}\,yr^{-1}$ (D'Hondt et al., 2009). In general nitrification rates in the oxic intervals near the seafloor were comparable to rates in the oxic layers near the underlying crust. The highest rates of denitrification typically coincided with depths having the lowest O_2, with the exception of rather low rates near the central anoxic zone of core 2B. Nitrification, which requires O_2, is observed as deep as 28 m in 2B and all the way to the underlying crust at the other two sites. Interestingly, modeled rates of nitrification were typically highest at comparatively low levels of dissolved O_2 (~ 15 µM in 2B, ~ 10 µM in 3D and ~ 35 µM in 4A) – suggesting an important role for micro-aerophilic nitrification. The depths of maximum denitrification rates generally coincided with the onset of O_2 levels below ~ 2 µM. In 2B, denitrification rates were highest at depths of ~ 28 and ~ 72 m (Fig. 3). In 3D, maximum denitrification rates were observed at 21 m – with similar rates between 20 and 25 m. Interestingly, the model indicated no denitrification within the 3 m anoxic zone of this core – suggesting limitation by organic substrate availability. In contrast, rates of denitrification were only estimated to occur within the anoxic zone of site 4A (e.g., not within the transitional intervals, although this was somewhat sensitive to prescribed $^{15}\varepsilon_{DNF}$, see below), with the highest rate of 24 $nmol\,cm^{-3}\,yr^{-1}$ at a depth of 44 m. Overall, rates of both nitri-

fication and denitrification were highest at site 2B and lowest in 4A, consistent with the putatively greater amount of microbial activity revealed by the sharper O_2 profile 2B. In all three cores maximum rates of nitrification exceeded those of denitrification, consistent with the net accumulation of NO_3^- throughout the sediment column. Even in 2B, where O_2 is below 2 µM over an interval of ~ 40 m, the NO_3^- concentration profile exhibits no obvious influence by NO_3^- reduction (Fig. 1).

Finally, the model suggests the co-occurrence of nitrification and denitrification (Fig. 3) in the transition zones of our model (depths at which O_2 is between 2 and 40 µM). Although denitrification rates generally did not exceed those of nitrification where the two processes are co-occurring (i.e., no net nitrate consumption), the increasing $\delta^{15}N$ and $\delta^{18}O$ of NO_3^- clearly reflects the influence of NO_3^- loss via denitrification. Indeed similar inferences have also been made about such overlap of nitrification and denitrification in the albeit much deeper and organic-rich hadopelagic sediments of the Ogasawara Trench (Nunoura et al., 2013). This observation illustrates the exceptionally extended vertical redox zonation of these sediments – and highlights the potential interaction between nitrogen transformations that are classically considered spatially explicit.

4.2.2 Model-predicted values of $\delta^{15}N_{NTR}$: implications for N sources and processes in oligotrophic sediments

In general, where NH_4^+ from remineralization does not accumulate – it is expected that the $\delta^{15}N$ of NO_3^- produced by NH_4^+ oxidation will be equivalent to the $\delta^{15}N$ of the NH_4^+ deriving from remineralization of organic nitrogen. The $\delta^{15}N$ of organic N of the North Pond sediments was not quantified in this study (concentrations are extremely low). Yet, the average model predicted $\delta^{15}N$ of newly produced NO_3^- ($\delta^{15}N_{NTR}$) (Fig. 4) ranged from −3.1 to +1.1‰ (standard error typically ±0.3 to 0.4‰), generally lower than that expected based on the $\delta^{15}N$ of sinking organic matter from the surface ocean of $\sim$ +3.7‰ (Altabet, 1988, 1989; Knapp et al., 2005; Ren et al., 2012). Values of

δ^{15}N$_{\text{NTR}}$ > +1‰ were only observed just above the O$_2$ minimum at sites 2B and 3D (Fig. 4).

Confronted with this difference, we turn to other factors that might play a role in setting the δ^{15}N$_{\text{NTR}}$. The lower δ^{15}N values of new NO$_3^-$ can potentially be explained by a number of possible processes including: (1) isotopic fractionation during remineralization, (2) competitive branching between NH$_4^+$ oxidation (whether anaerobic or aerobic) and NH$_4^+$ assimilation or (3) contribution of low δ^{15}N through organic matter derived from sedimentary N fixation.

Nitrogen isotope fractionation during organic matter remineralization has been reported (Altabet, 1988; Altabet et al., 1999; Estep and Macko, 1984; Lehmann et al., 2002), whereby the preferential remineralization of low δ^{15}N organic matter leads to production of low δ^{15}N NH$_4^+$ (which could feed into the production of low δ^{15}N NO$_3^-$). The influence of this phenomenon is more likely, however, during remineralization of fresh organic matter and where the heterotrophic community has abundant access to highly labile proteinaceous organic matter (Altabet, 1988; Estep and Macko, 1984). At North Pond, given the extremely low levels of organic material present in the sediments, it seems unlikely that preferential utilization of low δ^{15}N organic material during diagenesis is responsible for the low δ^{15}N$_{\text{NTR}}$.

Competitive branching of NH$_4^+$ supporting simultaneous nutritional supply (as an N source) and energy supply (via autotrophic ammonia oxidation) has been used to explain NO$_3^-$ dual isotopic composition in N rich surface waters (Wankel et al., 2007). Because N isotope fractionation during ammonia oxidation was argued to be stronger than that of NH$_4^+$ assimilation by phytoplankton under surface water conditions, it was argued that this competitive branching leads to a shunt of low δ^{15}N into the NO$_3^-$ pool via ammonia oxidation (Wankel et al., 2007). In contrast to the high-nutrient, sunlit, productive waters of Monterey Bay, however, under the energy-limited, and extremely low NH$_4^+$ production conditions in North Pond porewaters mechanisms of NH$_4^+$ partitioning are likely operating quite differently.

Full Screen / Esc

Printer-friendly Version

Interactive Discussion

Full Screen / Esc

Printer-friendly Version

Interactive Discussion

Although North Pond porewaters contain abundant NO_3^-, assimilation of NO_3^- as a nutritional N source requires an associated metabolic energy for reduction of NO_3^- (via an assimilatory nitrate reductase), a costly process in this energy poor environment. On the other hand, although NH_4^+ is more easily assimilated by most microbes, its exceedingly low abundance in North Pond porewaters reflect its scarcity as source of N required for cell growth. Based on the estimated values of the N isotope effect for NO_3^- consumption (by denitrification) in the porewaters of 2B that average $\sim 20\,‰$ (Table 2), there is little suggestion of NO_3^- assimilation, which would lead to much lower estimated values of $^{15}\varepsilon_{DNF}$ (Granger et al., 2010). Thus, it is more likely that nutritional N originates from a reduced form such as NH_4^+ and/or organic N. If the N isotope effect for ammonia oxidation is much larger than that of ammonia assimilation, then a competitive branching effect may also be contributing to a low $\delta^{15}N_{NTR}$. However, given such low concentrations, it is likely that microbial acquisition of NH_4^+ (whether for assimilation or for oxidation) is diffusion limited, conditions under which the N isotope effect is expected to be near $0\,‰$ (Hoch et al., 1992). Under such conditions very little isotopic fractionation should be realized and competitive branching seems an unlikely explanation for the low $\delta^{15}N_{NTR}$.

A final possibility for the low values of $\delta^{15}N_{NTR}$ could reflect the importance of benthic N-fixation operating at very low levels in North Pond sediments. Bacterial N-fixation is generally thought to result in biomass having a $\delta^{15}N$ between –2 and $0\,‰$ (Delwiche et al., 1979; Meador et al., 2007; Minigawa and Wada, 1986), which could effectively introduce new N and decrease bulk $\delta^{15}N$. Benthic N-fixation is not generally considered to be an important enough contribution to the total sediment organic matter to influence the bulk $\delta^{15}N$ values of sediment organic matter. However, given the low organic matter flux to these sediments from the overlying oligotrophic surface waters, a proportionately smaller amount of N-fixation would be required to significantly impact the sediment organic $\delta^{15}N$ value. While N-fixation is an energetically costly metabolism and might seem an unlikely strategy given the abundant porewater NO_3^- pool, it has been recently

acknowledged that N-fixation in benthic environments may be widely underestimated, despite high levels of porewater DIN including NO_3^- and/or NH_4^+ (Knapp, 2012).

In fact, N-fixation could be ecologically favored in organic-lean sediments like those at North Pond owing to the formation of H_2 as an end product, which might afford an energetic advantage in sediment microbial communities. For example, H_2 production could help to fuel autotrophic metabolisms including both NO_3^- reduction (e.g., Nakagawa et al., 2005) or the Knallgas reaction ($H_2 + O_2$). Hydrogen-based metabolism has been proposed as a significant support for subsurface autotrophy underlying the oligotrophic South Pacific Gyre (D'Hondt et al., 2009). Although the involvement of so-called alternative nitrogenases (the Fe and V forms), which have been shown to display an even larger kinetic isotope effect (−6 to −7‰) than the Mo-bearing form (Zhang et al., 2014), could offer even greater leverage on lowering of the bulk $\delta^{15}N$ (and source of N for nitrification), their involvement in non-sulfidic marine systems, where Mo is replete and soluble Fe and V is scarce, is expected to be minimal (Zhang et al., 2014). A similar argument was also made for the cryptic involvement of N fixation as source of low $\delta^{15}N$ and explanation for dual NO_3^- isotopic patterns in the large oxygen minimum zone of eastern tropical North Pacific (Sigman et al., 2005). Thus, we conclude that the low predicted values of $\delta^{15}N_{NTR}$ provide compelling evidence for an important role of in situ N-fixation in these organic matter depleted sediments.

Finally, there is a conspicuous increase in the predicted $\delta^{15}N_{NTR}$ at sites 2B and 3D (up to +1.8 and +1.1‰, respectively) between 15–35 m. Although we have no compelling explanation for these observations, it is interesting that these values coincide with the transitional intervals over which $\delta^{18}O_{NO_3}$ values increase much more rapidly than $\delta^{15}N_{NO_3}$. While it is possible that our model is insufficient for constraining the isotope dynamics at NP, it may also be that these suboxic depths support differential amounts of in situ nitrogen fixation leading to shifts in the bulk $\delta^{15}N$ available for oxidation by nitrification.

Full Screen / Esc

Printer-friendly Version

Interactive Discussion

4.2.3 Model predicted values of the δ^{18}O of nitrification ($\delta^{18}O_{NTR}$)

We also observed variation in estimated values of the δ^{18}O of newly produced NO_3^- ($\delta^{18}O_{NTR}$), ranging from −2.8 to as high as +4.1‰ (at the O_2 minimum in 3D), which may offer some insight into the nature of nitrification in these sediments and the deep ocean in general. The oxygen isotope composition of newly produced NO_3^- reflects the combination of several complex factors including (1) the δ^{18}O of the ambient water and dissolved O_2, (2) kinetic isotope effects during the enzymatically catalyzed incorporation of O atoms during oxidation of NH_4^+ and NO_2^-, as well as (3) the potential influence of oxygen isotope equilibration between water and NO_2^- (both abiotic and/or that catalyzed by activity of microbial nitrifying bacteria) (Casciotti et al., 2010).

In the upper profile of site 2B and throughout the profile of site 4A predicted values of $\delta^{18}O_{NTR}$ clustered between −2.8 and 0.0‰ with no clear trends related to down core concentrations of O_2 or NO_3^- (Fig. 5). Although slightly lower, this range of values agrees remarkably well with values predicted by experiments using a co-culture of NH_4^+ and NO_2^- oxidizing bacteria, which ranged from −1.5 to +1.3‰ (Buchwald et al., 2012). In systems where NH_4^+ and NO_2^- oxidizing bacteria co-exist and are not substrate-limited, NO_2^- does not generally accumulate and the importance of oxygen isotope equilibration between NO_2^- and water can be considered minor ($\sim 3\%$) (Buchwald et al., 2012). In this case, the $\delta^{18}O_{NTR}$ is primarily set by the δ^{18}O of water (seawater δ^{18}O ~ 0‰) and dissolved O_2 ($\sim +26.4$‰ for the deep N. Atlantic; Kroopnick et al., 1972) and the three kinetic isotope effects during the sequential oxidation of NH_4^+ to NO_3^- (Buchwald et al., 2012; Casciotti et al., 2010). The resulting $\delta^{18}O_{NTR}$ can be described as:

$$\delta^{18}O_{NTR} = 1/3\left[\delta^{18}O_{O_2} - \left(^{18}\varepsilon_{O_2}\right)\right] + 1/3\left[\delta^{18}O_{water} - \left(^{18}\varepsilon_{H_2O,1}\right)\right]$$
$$+ 1/3\left[\delta^{18}O_{water} - {}^{18}\varepsilon_{H_2O,2}\right] \tag{11}$$

where $^{18}\varepsilon$ is the kinetic isotope effect of O atom incorporation from O_2 during NH_4^+ oxidation to NH_2OH ($^{18}\varepsilon_{O_2}$), and from water during NH_2OH oxidation to NO_2^- ($^{18}\varepsilon_{H_2O,1}$) and NO_2^- oxidation to NO_3^- ($^{18}\varepsilon_{H_2O,2}$) (Buchwald et al., 2012).

While the value of seawater $\delta^{18}O$ can be considered to be relatively constant ($\sim 0\,‰$) in North Pond porewaters, the respiratory consumption of O_2, as evident in the observed concentration profiles, imparts a relatively strong isotopic fractionation (Bender, 1990; Kroopnick and Craig, 1976) and will cause elevated $\delta^{18}O_{O_2}$ values. Using a separate reaction-diffusion model (not shown) we estimated the $\delta^{18}O_{O_2}$ to be as high as $+70\,‰$ where concentrations of O_2 have been drawn down $> 95\,\%$ of the level found in bottom seawater. Incorporation of this highly ^{18}O-enriched O_2 by nitrification in these low O_2 intervals may contribute to observed increases in $\delta^{18}O_{NTR}$ predicted by our model. In particular, in the low O_2 intervals of 2B and 3D, $\delta^{18}O_{NTR}$ values as high as $+4.1\,‰$ at the four intervals coinciding with the maximum O_2 drawdown (Fig. 5), and thus may point to incorporation of high-$\delta^{18}O$ O_2. For example, assuming a $\delta^{18}O$ value of $0\,‰$ for seawater, using Eq. (11) and a combined isotope effect of $18\,‰$ for the two steps of NH_4^+ oxidation to NO_2^- ($^{18}\varepsilon_{O_2} + ^{18}\varepsilon_{H_2O,1}$; the two have not yet been resolved from one another; Casciotti et al., 2010) and a value of $15\,‰$ for $^{18}\varepsilon_{H_2O,2}$ (O atom incorporation during NO_2^- oxidation to NO_3^-, Buchwald et al., 2012), $\delta^{18}O_{NTR}$ values of -2, $+2$ or $+6\,‰$ would imply incorporation of O from an O_2 pool with a value of $\sim +45$, $+57$ or $+69\,‰$, respectively.

If these higher values are indeed the result of enriched O_2 incorporation, then they also provide indirect information on the degree of oxygen isotope equilibration occurring between NO_2^- and water. Specifically, if some proportion of an elevated $\delta^{18}O_{O_2}$ signal is propagated into the NO_3^- pool, then this suggests that the intermediate NO_2^- pool did not completely equilibrate with ambient water (which would effectively erase all signs of precursor molecule $\delta^{18}O$). Within these low O_2 transitional intervals in 2B and 3D, it appears that the turnover of the very small NO_2^- intermediate pool may be faster

than the time required for complete equilibration between NO_2^- and water (Buchwald and Casciotti, 2013). In contrast, the low O_2 interval from site 4A does not exhibit elevated $\delta^{18}O_{NTR}$ values near the oxygen minimum, perhaps suggesting that the turnover of NO_2^- here is slower (allowing complete equilibration) or that equilibration is biologically catalyzed. Although the concentrations of the NO_2^- pool were generally below detection, making the accurate determination of its turnover time impossible (via $\delta^{18}O$), the use of NO_2^- oxygen isotopes as an independent measure of metabolic processes where concentrations persist at measurable levels may be a potentially powerful indicator of biological turnover of NO_2^- ($\delta^{15}N$ and $\delta^{18}O$ of NO_2^- in 2B, where NO_2^- was detected at two depths, were not determined as part of this study). Future studies should target this pool as a complementary dimension for constraining subsurface biosphere metabolic rates.

4.2.4 Model sensitivity to prescribed $^{15}\varepsilon_{DNF}$ in transitional intervals

In the transitional intervals – where both nitrification and denitrification are allowed to co-occur, the model is underdetermined and requires some variables to be prescribed. We chose to prescribe a value for the kinetic isotope effect of denitrification ($^{15}\varepsilon_{DNF}$) and here examine the sensitivity of estimated rates nitrification and denitrification, as well as predicted values of $\delta^{15}N_{NTR}$ and $\delta^{18}O_{NTR}$. Given the rather tightly confined range of determined values for $^{15}\varepsilon_{DNF}$ in the anoxic zone of site 2B, averaging 20 ± 1.8‰, for illustration, we bracket our prescribed $^{15}\varepsilon_{DNF}$ in transitional intervals with values of 15 and 25‰ (rate estimates where the prescribed $^{15}\varepsilon_{DNF}$ is as low as 5‰ are given in Table 1). Overall, the model predicted rates of nitrification and denitrification, as well as values of $\delta^{15}N_{NTR}$ and $\delta^{18}O_{NTR}$ were largely insensitive to changes in the prescribed strength of the isotope effect for denitrification ($^{15}\varepsilon_{DNF}$) (Fig. 3).

Specifically, when the prescribed value of $^{15}\varepsilon_{DNF}$ decreased from 25 to 15‰, changes in the predicted values of $\delta^{15}N_{NTR}$ and $\delta^{18}O_{NTR}$ were generally small (Figs. 4 and 5), varying by a maximum of 0.9‰ (average 0.5‰) and 2.3‰ (difference 0.6‰),

respectively. An exception to this are the intervals bracketing the anoxic zone of the profile at site 2B (at depths of 27.9 and 70.8, 72.9 m), which yielded predicted $\delta^{15}N_{NTR}$ that were either 2.1 ‰ lower (at 27.9 m) or ~ 5 ‰ higher (at 70.8 and 72.9 m). Predicted $\delta^{18}O_{NTR}$ values were also quite sensitive to $^{15}\varepsilon_{DNF}$ in this interval with values that were 3.8 ‰ (at 27.9 m) and 7.2–8.0 ‰ higher (at 70.8 and 72.9 m). While we cannot rule out the potential influence of changes in physiological expression of isotope effects, the sensitivity of $\delta^{15}N_{NTR}$ and $\delta^{18}O_{NTR}$ to $^{15}\varepsilon_{DNF}$ at these depths may point to an unresolvable artifact of this model approach. Further work being indicated, incorporation of dual nitrite isotopes could certainly aid in resolving this apparent sensitivity. However, this sensitivity was not observed in the other transitional intervals of 2B, 3D or 4A and conclusions regarding $\delta^{15}N_{NTR}$ and $\delta^{18}O_{NTR}$ still appear robust.

Finally, although literature values of $^{15}\varepsilon_{DNF}$ almost uniformly fall between values of 13 and 30 ‰, values of $^{15}\varepsilon_{DNF}$ as low as 2–5 ‰ have been observed occasionally in culture studies (Granger et al., 2008; Wada et al., 1975). While we have no direct evidence that such low values would be relevant in our study, we report the sensitivity of rate estimates and $\delta^{15}N_{NTR}$ and $\delta^{18}O_{NTR}$ (Table 1). In short, a prescribed value for $^{15}\varepsilon_{DNF}$ of 5 ‰ lead to increased estimates of $\delta^{15}N_{NTR}$ and $\delta^{18}O_{NTR}$ by an average of 2.3 and 1.4 ‰, respectively (Figs. 4 and 5). These higher estimates of $\delta^{15}N_{NTR}$ would implicitly require a lower contribution of N-fixation derived nitrogen as argued for above, though not eliminate its role completely, especially in 4A where $\delta^{15}N_{NTR}$ values remain between −1 to +1 ‰ (Fig. 4).

While rates of nitrification were less sensitive (somewhat higher in the upper layers of 4A), this very low prescribed value of $^{15}\varepsilon_{DNF}$ often lead to dramatically increased estimates of denitrification rates – in particular in the upper transitional layers of profiles at 2B and 3D where maximum denitrification rates increased ~ 10–20 fold (Table 1). This sensitivity of denitrification to $^{15}\varepsilon_{DNF}$ values makes intuitive sense, since more denitrification would be required to generate the strongly elevated $\delta^{15}N$ and $\delta^{18}O$ values observed in 2B and 3D.

4.2.5 Model predicted values of $^{18}\varepsilon{:}^{15}\varepsilon_{DNF}$ and $^{15}\varepsilon_{DNF}$

In the anoxic intervals, estimated values of $^{18}\varepsilon{:}^{15}\varepsilon_{DNF}$ ranged from 0.83 to 1.11 with an average value of 0.99 ± 0.1 (Table 2), consistent with a prominent role of respiratory nitrate reductase (Nar), which imparts a $^{18}\varepsilon{:}^{15}\varepsilon_{DNF}$ of $\sim 0.96 \pm 0.01$ (Granger et al., 2008). Notably, however, the lower values of 0.86 and 0.83 observed near the top and the core of the anoxic zone in site 2B could suggest influence of nitrate reduction by periplasmic nitrate reductase (NAP) (Granger et al., 2008) or chemolithotrophic NO_3^- reduction (Frey et al., 2014; Wenk et al., 2014), which has been shown to impart a lower $^{18}\varepsilon{:}^{15}\varepsilon_{DNF}$ closer to 0.6. In this particular interval, this could suggest that as much as 43 % of nitrate reduction is chemolithotrophic and perhaps metabolically linked to the oxidation of inorganic substrates such as reduced iron or sulfur species. Although outside the scope of this study, interrogation of genetic markers of respiratory and periplasmic nitrate reductase could shed more light on the role nitrate use by subsurface microbial communities.

As discussed above, the model-estimated values of $^{15}\varepsilon_{DNF}$ (averaging 20.0 ± 1.8‰; Table 2) at site 2B are quite consistent with values from a wide range of studies (Granger et al., 2008), and references therein). Notably however, a different pattern emerges from the two anoxic intervals of site 4A. Although model-estimated values of $^{15}\varepsilon_{DNF}$ were unresolvable at 38.8 m (likely because the changes in $\delta^{15}N$ and $\delta^{18}O$ were too small for reliable model fits), estimated $^{15}\varepsilon_{DNF}$ values at 44.1 m were $\sim 8.1 \pm 0.4$ ‰, much lower than observed in 2B. In general, the values observed in 2B are consistent with observations from other environments hosting denitrification (e.g., OMZs, soils, groundwater aquifers, etc.) (Granger et al., 2008), and references therein), and suggest that denitrifying organisms may be adapted to low levels of carbon and that their physiological poise may be similar to those found in other anaerobic environments (albeit adapted to grow at exceedingly slow nitrate reduction rates). However, the lower estimated $^{15}\varepsilon_{DNF}$ values in 4A might also reflect something more. Given the apparent low reactivity of the sediments of site 4A, it is also possible that these particularly low

$^{15}\varepsilon_{DNF}$ values stem from denitrification operating under extreme physiological energy limitation – as discussed below.

While a number of studies have shown that the apparent N isotopic effect for nitrate reduction by denitrification can vary from 5 to 30‰ (e.g., Barford et al., 1999; Delwiche and Steyn, 1970; Granger et al., 2008), recent evidence suggests these variations are largely regulated by changes in the combination of cellular uptake and efflux of NO_3^- leading to the expression (or repression) of the enzyme level isotope effect outside the cell (Granger et al., 2008; Kritee et al., 2012; Needoba et al., 2004). For example, at low extracellular NO_3^- concentrations – low $^{15}\varepsilon_{DNF}$ values suggest that nitrate transport (having a low $^{15}\varepsilon$) becomes the rate-limiting step (Granger et al., 2008; Lehmann et al., 2007; Shearer et al., 1991). In North Pond porewaters, however, at depths where O_2 is low enough for denitrification to occur, NO_3^- concentrations remain well above 30 µM, a threshold well above the K_m for NO_3^- transporters (2–18 µM; Parsonage et al., 1985; Murray et al., 1989; Zumft, 1997), suggesting that low $^{15}\varepsilon_{DNF}$ due to transport limitation of NO_3^- reduction is unlikely.

In general, greater expression of the intrinsic enzymatic isotope effect (e.g., higher observed $^{15}\varepsilon_{DNF}$) should occur under conditions in which there is a higher efflux of intracellular NO_3^- relative to NO_3^- uptake (Kritee et al., 2012). Interestingly, this efflux/uptake ratio appears to be linked to nitrate reduction rates in denitrifying bacteria, with lower cell-specific nitrate reduction rates leading to lower efflux/uptake ratios and lower observed cellular level $^{15}\varepsilon_{DNF}$ (Kritee et al., 2012). Indeed, evidence seems to indicate that this efflux/uptake ratio in denitrifying bacteria is highly regulated and that NO_3^- uptake is sensitive to cellular level energy supply. For example, under conditions in which organisms are required to maintain a careful regulation of energetically costly metabolic processes, it is logical that there would be a lower density of NO_3^- transporters and that intracellular NO_3^- concentrations would be maintained at or near optimal levels for reduction by nitrate reductase. Similarly, growth under energy-poor carbon substrate supply may also lead to lower observed $^{15}\varepsilon_{DNF}$, due to an energy-

13573

driven decrease in NO_3^- uptake, lower intracellular NO_3^- concentrations and a lower efflux/uptake ratio.

We suggest that the difference between the lower $^{15}\varepsilon_{DNF}$ value estimated from the anoxic interval of 4A and the more "conventional" values from deeper within anoxic

5 intervals of 2B could stem from physiological-level controls on the cellular level expression of $^{15}\varepsilon_{DNF}$. Specifically, as all porewater evidence from site 4A (O_2, NO_3^-, N and O isotopes) indicates substantially lower levels of microbial activity, denitrification may actually be more energy-limited by carbon (compared to denitrification in the deeper intervals of 2B). This suggests that the operation of denitrification under ex-

10 tremely carbon-poor environments (4A) may lead to conditions where the enzyme-level N isotope fractionation of denitrification is under-expressed on the cellular, and hence ecosystem level, and $^{15}\varepsilon_{DNF}$ values are much lower than commonly encountered under even just slightly more energy-replete conditions (e.g., 2B).

5 Summary

15 In summary, the porewater nitrate isotopic composition reflects the active redox cycling of nitrogen by the subsurface microbial community – including both oxidative and reductive transformations. The variations in reaction rates across and within the three North Pond sites are generally consistent with the distribution of dissolved oxygen, but not necessarily with the canonical view of how redox thresholds act to spatially

20 separate nitrate regeneration from dissimilatory consumption (e.g., denitrification). The incorporation of nitrate dual isotopes into an inverse reaction-diffusion model provides evidence for extensive zones of overlap where O_2 and NO_3^- respiration (nitrification and denitrification) co-occur. The isotope modeling also yielded estimates for the $\delta^{15}N$ and $\delta^{18}O$ of newly produced nitrate ($\delta^{15}N_{NTR}$ and $\delta^{18}O_{NTR}$), as well as the isotope effect

25 for denitrification ($^{15}\varepsilon_{DNF}$), parameters with high relevance to global ocean models of N cycling. Estimated values of $\delta^{15}N_{NTR}$ were generally lower than previously reported

Printer-friendly Version

Interactive Discussion

δ^{15}N values for sinking PON in this region, suggesting the potential influence of sedimentary N-fixation and remineralization/oxidation of the newly fixed organic N. Model estimated values of $\delta^{18}O_{NTR}$ generally ranged between –2.8 and 0.0‰, consistent with lab studies of nitrifying bacteria cultures. Notably, however, some $\delta^{18}O_{NTR}$ values were elevated, suggesting incorporation of ^{18}O-enriched dissolved oxygen during the nitrification process, and implying relatively rapid rates of nitrite turnover in environments supporting nitrification. In contrast, the accumulation of NO_2^- under denitrifying conditions likely reflects limitation of NO_2^- by organic matter availability and generally low rates of N based heterotrophic respiration. Importantly, our findings indicate that the production of organic matter by in situ autotrophy (e.g., nitrification and nitrogen fixation) must supply a large fraction of the biomass and organic substrate for heterotrophy in these sediments, supplementing the small organic matter pool derived from the overlying euphotic zone. Thus, this work sheds new light on an active nitrogen cycle operating, despite exceedingly low carbon inputs, in the deep sedimentary biosphere underlying half of the global ocean.

References

Altabet, M. A.: Variations in nitrogen isotopic compostion between sinking and suspended particles: implications for nitrogen cycling and particle transformations in the open ocean, Deep-Sea Res. Pt. I, 35, 535–554, 1988.

Altabet, M. A.: A time-series study of the vertical structure of nitrogen and particle dynamics in the Sargasso Sea, Limnol. Oceanogr., 34, 1185–1201, 1989.

Altabet, M. A., Pilskaln, C., Thunell, R. C., Pride, C., Sigman, D. M., Chavez, F. P., and Francois, R.: The nitrogen isotope biogeochemistry of sinking particles from the margin of the Eastern North Pacific, Deep-Sea Res. Pt. I, 46, 655–679, 1999.

Andersson, K. K. and Hooper, A. B.: O_2 and H_2O are each the source of one O in NO_2 produced from NH_3 by Nitrosomonas: ^{15}N-NMR evidence, FEBS Lett., 164, 236–240, 1983.

Barford, C. C., Montoya, J. P., Atlabet, M. A., and Mitchell, R.: Steady-state nitrogen isotope effects of N_2 and N_2O production in paracoccus denitrificans, Appl. Environ. Microb., 65, 989–994, 1999.

Becker, K., Bartetzko, A., and Davis, E. E.: Revisiting Hole 395A for Logging and Long-term Monitoring of Off-axis Hydrothermal Processes in Young Ocean Crust, Proceedings of the Ocean Drilling Program, Scientific Results, Volume 174B, 1–13, 2001.

Bender, M. L.: The δ^{18}O of dissolved O_2 in seawater: A unique tracer of circulation and respirationin the deep sea, J. Geophys. Res., 95, 22243–22252, 1990.

Berelson, W. M., Hammond, D. E., O'Neill, D., Xu, X.-M., Chin, C., and Zukin, J.: Benthic fluxes and pore water studies from sediments of the central equatorial north Pacific: nutrient diagenesis, Geochim. Cosmochim. Ac., 54, 3001–3012, 1990.

Blair, N. E. and Aller, R. C.: The fate of terrestrial organic carbon in the marine environment, Ann. Rev. Mar. Sci., 4, 401–423, doi:10.1146/annurev-marine-120709-142717, 2012.

Braman, R. S. and Hendrix, S. A.: Nanogram nitrite and nitrate determination in environmental and biological materials by vanadium (III) reduction with chemiluminescence detection, Anal. Chem., 61, 2715–2718, 1989.

Buchwald, C. and Casciotti, K. L.: Oxygen isotopic fractionation and exchange during bacterial nitrite oxidation, Limnol. Oceanogr., 55, 1064–1074, 2010.

Buchwald, C. and Casciotti, K. L.: Isotopic ratios of nitrite as tracers of the sources and age of oceanic nitrite, Nat. Geosci., 6, 309–313, 2013.

5 Buchwald, C., Santoro, A. E., McIlvin, M. R., and Casciotti, K. L.: Oxygen isotopic composition of nitrate and nitrite produced by nitrifying cocultures and natural marine assemblages, Limnol. Oceanogr., 57, doi:10.4319/lo.2012.57.5.1361, 2012.

Casciotti, K. L. and McIlvin, M. R.: Isotopic analyses of nitrate and nitrite from reference mixtures and application to Eastern Tropical North Pacific waters, Mar. Chem., 107, 184–201, 10 2007.

Casciotti, K. L., Sigman, D. M., Galanter-Hastings, M., Böhlke, J. K., and Hilkert, A.: Measurement of the oxygen isotopic composition of nitrate in seawater and freshwater using the denitrifier method, Anal. Chem., 74, 4905–4912, 2002.

Casciotti, K. L., Trull, T. W., Glover, D., and Davies, D.: Constraints on nitrogen cycling at the 15 subtropical North Pacific Station ALOHA from isotopic measurements of nitrate and particulate nitrogen, Deep-Sea Res. Pt. II, 55, 1661–1672, 2008.

Casciotti, K. L., McIlvin, M., and Buchwald, C.: Oxygen isotopic exchange and fractionation during bacterial ammonia oxidation, Limnol. Oceanogr., 55, 753–762, 2010.

Christensen, J. P. and Rowe, G. T.: Nitrification and oxygen consumption in northwest Atlantic 20 deep-sea sediments, J. Mar. Res., 42, 1099–1116, 1984.

Christensen, J. P., Murray, J. W., Devol, A. H., and Codispoti, L. A.: Denitrification in continental shelf sediments has major impact on the ocean nitrogen budget, Global Biogeochem. Cy., 1, 97–116, 1987.

Clark, I. and Fritz, P.: Environmental Isotopes in Hydrogeology, CRC Press, Boca Raton, 25 Florida, 331 pp., 1997.

D'Hondt, S., Spivack, A. J., Pockalny, R., Ferdelman, T. G., Fischer, J. P., Kallmeyer, J., Abrams, L. J., Smith, D. C., Graham, D., Hasiuk, F., Schrum, H., and Stancin, A. M.: Subseaflor sedimentary life in the South Pacific Gyre, P. Natl. Acad. Sci. USA, 106, 11651–11656, 2009.

30 D'Hondt, S., Inagaki, F., Zarikian, C. A., Abrams, L. J., Dubois, N., Engelhardt, T., Evans, H., Ferdelman, T., Gribsholt, B., Harris, R. N., Hoppie, B. W., Hyun, J.-H., Kallmeyer, J., Kim, J., Lynch, J. E., McKinley, C. C., Mitsunobu, S., Morono, Y., Murray, R. W., Pockalny, R., Sauvage, J., Shimono, T., Shiraishi, F., Smith, D. C., Smith-Duque, C. E., Spivack, A. J.,

Nitrogen cycling in deep-sea porewaters

S. D. Wankel et al.

Steinsbu, B. O., Suzuki, Y., Szpak, M., Toffin, L., Uramoto, G., Yamaguchi, Y. T., Zhang, G.-l., Zhang, X.-H., and Ziebis, W.: Presence of oxygen and aerobic communities from sea floor to basement in deep-sea sediments, Nat. Geosci., 8, 299–303, 2015.

Davis, E. E., Becker, K., Pettigrew, T., Carson, B., and MacDonald, R.: CORK: A Hydrological Seal and Downhole Observatory for Deep-Ocean Boreholes, Proceedings of the Ocean Drilling Program, Initial Results, Volume 139, 43–53, 1992.

Delwiche, C. C. and Steyn, P. L.: Nitrogen isotope fractionation in soils and microbial reactions, Environ. Sci. Technol., 4, 929–935, 1970.

Delwiche, C., Zinke, P., Johnson, C., and Virginia, R.: Nitrogen isotope distribution as a presumptive indicator of nitrogen-fixation, Bot. Gaz., 140, 65–69, 1979.

Devol, A. H.: Direct measurement of nitrogen gas fluxes from continental shelf sediments, Nature, 349, 319–321, 1991.

Edwards, K. J., Wheat, C. G., and Sylvan, J. B.: Under the sea: microbial life in volcanic oceanic crust, Nat. Rev. Microbiol., 9, 703–712, 2011.

Edwards, K. J., Bach, W., Klaus, A., and Scientists, E.: Mid-Atlantic Ridge Microbiology: Initiation of Long-Term Coupld Microbiological, Geochemical, and Hydrological Experimentation within the Seafloor at North Pond, Western Flank of the Mid-Atlantic Ridge, Integrated Ocean Drilling Program Management International, Inc., Tokyo, Japan, 2012a.

Edwards, K. J., Becker, K., and Colwell, F.: The deep, dark energy biosphere: intraterrestrial life on Earth, Ann. Rev. Earth Pl. Sc., 40, 551–568, doi:10.1146/annurev-earth-042711-105500, 2012b.

Estep, M. L. F. and Macko, S. A.: Nitrogen isotope biogeochemistry of thermal springs, Org. Geochem., 6, 779–785, 1984.

Expedition-336-Scientists: Mid-Atlantic Ridge microbiology: initiation of long-term coupled microbiological, geochemical and hydrological experimentation within the seafloor at North Pond, Western Flank of the Mid-Atlantic Ridge, Proceedings of the Ocean Drilling Program, Volume 336, 2012a.

Expedition-336-Scientists: Expedition 336 Summary, Tokyo, Japan, 2012b.

Fawcett, S. E., Ward, B. B., Lomas, M. W., and Sigman, D. M.: Vertical decoupling of nitrate assimilation and nitrification in the Sargasso Sea, Deep-Sea Res. Pt. I, 103, 64–72, 2015.

Fischer, J. P., Ferdelman, T. G., D'Hondt, S., Røy, H., and Wenzhöfer, F.: Oxygen penetration deep into the sediment of the South Pacific gyre, Biogeosciences, 6, 1467–1478, doi:10.5194/bg-6-1467-2009, 2009.

Nitrogen cycling in deep-sea porewaters

S. D. Wankel et al.

Frey, C., Heitanen, S., Jürgens, K., Labrenz, M., and Voss, M.: N and O isotope fractionation in nitrate during chemolithoautotrophic denitrification by Sulfurimonas gotlandica, Environ. Sci. Technol., 48, 13229–13327, doi:10.1021/es503456g, 2014.

Goloway, F. and Bender, M. L.: Diagenetic models of interstitial nitrate profiles in deep sea suboxic sediments, Limnol. Oceanogr., 27, 624–638, 1982.

Granger, J. and Sigman, D. M.: Removal of nitrite with sulfamic acid for nitrate N and O isotope analysis with the denitrifier method, Rapid Commun. Mass Sp., 23, 3753–3762, 2009.

Granger, J., Sigman, D. M., Needoba, J. A., and Harrison, P. J.: Coupled nitrogen and oxygen isotope fractionation of nitrate during assimilation by cultures of marine phytoplankton, Limnol. Oceanogr., 49, 1763–1773, 2004.

Granger, J., Sigman, D. M., Lehmann, M. F., and Tortell, P. D.: Nitrogen and oxygen isotope fractionation during dissimilatory nitrate reduction by denitrifying bacteria, Limnol. Oceanogr., 53, 2533–2545, 2008.

Granger, J., Sigman, D. M., Rohde, M., Maldonado, M., and Tortell, P. D.: N and O isotope effects during nitrate assimilation by unicellular prokaryotic and eukaryotic plankton cultures, Geochim. Cosmochim. Ac., 74, 1030–1040, 2010.

Granger, J., Prokopenko, M. G., Sigman, D. M., Mordy, C. W., Morse, Z. M., Morales, L., Sambrotto, R. N., and Plessen, B.: Coupled nitrification-denitrification in sediment of the eastern Bering Sea shelf leads to ^{15}N enrichment of fixed N in shelf waters, J. Geophys. Res., 116, C11006, doi:10.1029/2010JC006751, 2011.

Grasshoff, K., Kremling, K., and Ehrhardt, M.: Methods of Seawater Analysis, 3rd Edn., Wiley-VCH Verlag, GmbH, Weinheim, Germany, 2007.

Gruber, N.: The marine nitrogen cycle overview and challenges, in: Nitrogen in the Marine Environment, 2nd ed., edited by: Capone, D. G., Bronk, D. A., Mulholland, M. R., and Carpenter, E. J., Elsevier, Amsterdam, Netherlands, 1–50, 2008.

Grundmanis, V. and Murray, J. W.: Aerobic respiration of pelagic marine sediments, Geochim. Cosmochim. Ac., 46, 1101–1120, 1982.

Hammond, D. E., McManus, J., Berelson, W. M., Kilgore, T. E., and Pope, R. H.: Early diagenesis of organic material in equatorial Pacific sediments: stoichiometry and kinetics, Deep-Sea Res. Pt. II, 43, 1365–1412, 1996.

Hoch, M. P., Fogel, M. F., and Kirchman, D. L.: Isotope fractionation associated with ammonium uptake by a marine bacterium, Limnol. Oceanogr., 37, 1447–1459, 1992.

Nitrogen cycling in deep-sea porewaters

S. D. Wankel et al.

Jahnke, R. A., Emerson, S. R., and Murray, J. W.: A model of oxygen reduction, denitrification, and organic matter mineralization in marine sediments, Limnol. Oceanogr., 27, 610–623, 1982.

Karsh, K. L., Granger, J., Kritee, K., and Sigman, D. M.: Eukaryotic assimilatory nitrate reductase fractionates N and O isotopes with a ratio near unity, Environ. Sci. Technol., 46, 5727–5735, doi:10.1021/es204593q, 2012.

Knapp, A. N.: The sensitivity of marine N2 fixation to dissolved inorganic nitrogen, Frontiers in Microbiology, 3, p. 374, doi:10.3389/fmicb.2012.00374, 2012.

Knapp, A. N., Sigman, D. M., and Lipschultz, F.: N isotopic composition of dissolved organic nitrogen and nitrate at the Bermuda Atlantic Time-series Study site, Global Biogeochem. Cy., 19, doi:10.1029/2004GB002320, 2005.

Kritee, K., Sigman, D. M., Granger, J., Ward, B. B., Jayakumar, A., and Deutsch, C.: Reduced isotope fractionation by denitrificaiton under conditions relevant to the ocean, Geochim. Cosmochim. Ac., 92, 243–259, 2012.

Kroopnick, P. and Craig, H.: Oxygen isotope fractionation in dissolved oxygen in the deep sea, Earth Planet. Sc. Lett., 32, 375–388, 1976.

Kroopnick, P., Weiss, R. F., and Craig, H.: Total CO_2, ^{13}C, and dissolved oxygen ^{18}O at GEOSECS II in the North Atlantic, Earth Planet. Sc. Lett., 16, 103–110, 1972.

Langseth, M. G., Becker, K., von Herzen, R. P., and Schultheiss, P.: Heat and fluid flux through sediment on the western flank of the Mid-Atlantic Ridge: a hydrogeological study of North Pond, Geophys. Res. Lett., 19, 517–520, doi:10.1029/92GL00079, 1992.

Lehmann, M. F., Bernasconi, S. M., Barbieri, A., and McKenzie, J. A.: Preservation of organic matter and alteration of its carbon and nitorgen isotope composition during simulated and in situ early sedimentary diagenesis, Geochim. Cosmochim. Ac., 66, 3573–3584, 2002.

Lehmann, M. F., Sigman, D. M., and Berelson, W. M.: Coupling the $^{15}N/^{14}N$ and $^{18}O/^{16}O$ of nitrate as a constraint on benthic nitrogen cycling, Mar. Chem., 88, 1–20, 2004.

Lehmann, M. F., Sigman, D. M., McCorkle, D. C., Brunnelle, B. G., Hoffman, S., Kienast, M., Cane, G., and Clement, J.: Origin of the deep Bering Sea nitrate deficit: constraints from the nitrogen and oxygen isotopic composition of water column nitrate and benthic nitrate fluxes, Global Biogeochem. Cy., 19, GB4005, doi:10.1029/2005GB002508, 2005.

Lehmann, M. F., Sigman, D. M., McCorkle, D. C., Granger, J., Hoffman, S., Cane, G., and Brunelle, B. G.: The distribution of nitrate 15N/14N in marine sediments and the impact of

Title Page

Abstract | Introduction

Conclusions | References

Tables | Figures

|◄ | ►|

◄ | ►

Back | Close

Full Screen / Esc

Printer-friendly Version

Interactive Discussion

benthic nitrogen loss on the isotopic composition of oceanic nitrate, Geochim. Cosmochim. Ac., 71, 5384–5404, 2007.

Li, Y.-H. and Gregory, S.: Diffusion of ions in sea water and in deep-sea sediments, Geochim. Cosmochim. Ac., 38, 703–714, 1974.

5 Marconi, D., Weigand, M. A., Rafter, P. A., McIlvin, M. R., Forbes, M., Casciotti, K. L., and Sigman, D. M.: Nitrate isotope distributions on the US GEOTRACES North Atlantic cross-basin section: signals of polar nitrate sources and low latitude nitrogen cycling, Mar. Chem., in press, 2015.

Mason, O. U., Nakagawa, T., Rosner, M., van Nostrand, J. D., Zhou, J., Maruyama, A.,
10 Fisk, M. R., and Giovannoni, S. J.: First investigation of the microbiology of the deepest layer of ocean crust, PLoS One, 5, e15399, doi:10.1371/journal.pone.0015399, 2010.

McIlvin, M. and Casciotti, K. L.: Technical updates to the bacterial method for nitrate isotopic analyses, Anal. Chem., 83, 1850–1856, 2011.

McIlvin, M. R. and Casciotti, K. L.: Fully automated system for stable isotopic analyses of dis-
15 solved nitrous oxide at natural abundance levels, Limnol. Oceanogr.-Meth., 8, 54–66, 2010.

McManus, J., Hammond, D. E., Berelson, W. M., Kilgore, T. E., Demaster, D. J., Ragueneau, O. G., and Collier, R. W.: Early diagenesis of biogenic opal: dissolution rates, kinetics, and paleoceanographic implications, Deep-Sea Res. Pt. II, 42, 871–903, 1995.

Meador, T. B., Aluwihare, L. I., and Mahaffey, C.: Isotopic heterogeneity and cycling of organic
20 nitrogen in the oligotrophic ocean, Limnol. Oceanogr., 52, 934–947, 2007.

Minigawa, M. and Wada, E.: Nitrogen isotope ratios of red tide organisms in the East China Sea: a characterization of biological nitrogen fixation, Mar. Chem., 19, 245–259, 1986.

Murray, J. W. and Grundmanis, V.: Oxygen consumption in pelagic marine sediments, Science, 209, 1527–1530, 1980.

25 Murray, R., Parsons, L., and Smith, M.: Kinetics of nitrate utilization by mixed populations of denitrifying bacteria, Appl. Environ. Microb., 55, 717–721, 1989.

Nakagawa, S., Takai, K., Inagaki, F., Horikoshi, K., and Sako, Y.: Nitratiruptor tergarcus gen. no., sp. nov., and Nitratifractor salsuginis gen. nov., sp. nov., nitrate-reducing chemolithoautotrophs of the ε-Proteobacteria isolated from a deep-sea hydrothermal system in the Mid-
30 Okinawa Trough, Int. J. Syst. Evol. Micr., 55, 925–933, 2005.

Needoba, J. A., Sigman, D. M., and Harrison, P. J.: The mechanism of isotope fractionation during algal nitrate assimilation as illuminated by the 15N/14N of intracellular nitrate, J. Phycol., 40, 517–522, 2004.

Nitrogen cycling in deep-sea porewaters

S. D. Wankel et al.

⏮ | ⏭

◀ | ▶

Back | Close

Full Screen / Esc

Printer-friendly Version

Interactive Discussion

Nunoura, T., Nishizawa, M., Kikuchi, T., Tsubouchi, T., Hirai, M., Koide, O., Miyazaki, J., Hirayama, H., Koba, K., and Takai, K.: Molecular biological and isotopic biogeochemical prognoses of the nitrification-driven dynamic microbial nitrogen cycle in hadopelagic sediments, Environ. Microbiol., 15, 3087–3107, doi:10.1111/1462-2920.12152, 2013.

Orcutt, B. N., Sylvan, J. B., Knab, N. J., and Edwards, K. J.: Microbial ecology of the dark ocean above, at, and below the Seafloor, Microbiol. Mol. Biol. R., 75, 361–422, 2011.

Orcutt, B. N., Wheat, C. G., Rouxel, O., Hulme, S., Edwards, K. J., and Bach, W.: Oxygen consumption in subseafloor basaltic crust, Nature Communications, 4, 2539, doi:10.1038/ncomms3539, 2013.

Parsonage, D., Greenfield, A. J., and Ferguson, S. J.: The high affinity of Paracoccus denitrificans cells for nitrate as an electron acceptor. Analysis of possible mechanisms of nitrate and nitrite movement across the plasma membrane and the basis for inhibition by added nitrite of oxidase activity in permeabilised cells, Biochim. Biophys. Acta, 807, 81–95, 1985.

Picard, A. and Ferdelman, T.: Linking microbial heterotrophic activity and sediment lithology in oxic, oligotrophic sub-seafloor sediments of the North Atlantic Ocean, Frontiers in Microbiology, 2, 263, doi:10.3389/fmicb.2011.00263, 2011.

Prokopenko, M. G., Hirst, M., DeBrabandere, L., Lawrence, D., Berelson, W. M., Granger, J., Chang, B., Dawson, S. C., Crane III, E., Chong, L., Thamdrup, B., Townsend-Small, A., and Sigman, D. M.: Nitrogen losses in anoxic marine sediments driven by Thioploca-anammox bacteria consortia, Nature, 500, 194–198, doi:10.1038/nature12365, 2013.

Rabalais, N. N.: Nitrogen in aquatic environments, Ambio, 31, 102–112, 2002.

Ren, H., Sigman, D. M., Thunell, R. C., and Prokopenko, M. G.: Nitrogen isotopic composition of planktonic foraminifera from the modern ocean and recent sediments, Limnol. Oceanogr., 57, 1011–1024, 2012.

Risgaard-Petersen, N.: Coupled nitrification-denitrification in autotrophic and heterotrophic estuarine sediments: on the influence of benthic microalgae, Limnol. Oceanogr., 48, 93–105, 2003.

Røy, H., Kallmeyer, J., Adhikari, R. R., Pockalny, R., Jorgensen, B. B., and D'Hondt, S.: Aerobic microbial respiration in 86-million-year-old deep-sea red clay, Science, 336, 922–925, doi:10.1126/science.1219424, 2012.

Rutgers van der Loeff, M., Meadows, P., and Allen, J.: Oxygen in porewaters of deep-sea sediments [and Discussion], Philos. T. R. Soc. B, 331, 69–84, 1990.

Title Page

Abstract | Introduction

Conclusions | References

Tables | Figures

◄ | ►

◄ | ►

Back | Close

Full Screen / Esc

Printer-friendly Version

Interactive Discussion

Sachs, O., Sauter, E., Schlüter, M., Rutgers van der Loeff, M. M., Jerosch, K., and Holby, O.: Benthic organic carbon flux and oxygen penetration reflect different plankton provinces in the Southern Ocean, Deep-Sea Res. Pt. I, 56, 1319–1335, 2009.

Seeberg-Elverfeldt, J., Schlüter, M., Feseker, T., and Kölling, M.: Rhizon sampling of porewaters near the sediment–water interface of aquatic systems, Limnol. Oceanogr.-Meth., 3, 361–371, 2005.

Seitzinger, S. P., Nixon, S. W., and Pilson, M. E. Q.: Denitrification and nitrous oxide production in a coastal marine ecosystem, Limnol. Oceanogr., 29, 73–83, 1984.

Shearer, G. B., Schneider, J. D., and Kohl, D. H.: Separating the efflux and influx components of net nitrate uptake by Synechococcus R2 under steady-state conditions, J. Gen. Microbiol., 137, 1179–1184, 1991.

Sigman, D. M., Casciotti, K. L., Andreani, M., Barford, C., Galanter, M., and Böhlke, J. K.: A bacterial method for the nitrogen isotopic analysis of nitrate in seawater and freshwater, Anal. Chem., 73, 4145–4153, 2001.

Sigman, D. M., Granger, J., DiFiore, P. J., Lehmann, M. F., Ho, R., Cane, G., and van Geen, A.: Coupled nitrogen and oxygen isotope measurements of nitrate along the eastern North Pacific margin, Global Biogeochem. Cy., 19, GB4022, doi:10.1029/2005GB002458, 2005.

Wada, E., Kadonaga, T., and Matsuo, S.: 15N abundance in nitrogen of naturally occurring substances and global assessment of denitrification from isotopic viewpoint, Geochem. J., 9, 139–148, 1975.

Wankel, S. D., Kendall, C., Pennington, J. T., Chavez, F. P., and Paytan, A.: Nitrification in the euphotic zone as evidenced by nitrate dual isotopic composition: observations from Monterey Bay, California, Global Biogeochem. Cy., 21, GB2009, doi:10.1029/2006gb002723, 2007.

Wankel, S. D., Kendall, C., and Paytan, A.: Using nitrate dual isotopic composition (δ^{15}N and δ^{18}O) as a tool for exploring sources and cycling of nitrate in an estuarine system: elkhorn Slough, California, J. Geophys. Res., 114, G01011, doi:10.1029/2008JG000729, 2009.

Wenk, C. B., Zopfi, J., Blees, J., Veronesi, M., Niemann, H., and Lehmann, M. F.: Community N and O isotope fractionaiton by sulfide-dependent denitrificaiton and anammox in a stratified lacustrine water column, Geochim. Cosmochim. Ac., 125, 551–563, doi:10.1016/j.gca.2013.10.034, 2014.

Zhang, X., Sigman, D. M., Morel, F. M. M., and Kraepiel, A. M. L.: Nitrogen isotope fractionation by alternative nitrogenases and past ocean anoxia, P. Natl. Acad. Sci. USA, 111, 4782–4787, 2014.

Ziebis, W., McManus, J., Ferdelman, T., Schmidt-Schierhorn, F., Bach, W., Muratli, J., Edwards, K. J., and Villinger, H.: Interstitial fluid chemistry of sediments underlying the North Atlantic Gyre and the influence of subsurface fluid flow, Earth Planet. Sc. Lett., 323–324, 79–91, 2012.

Zumft, W. G.: Cell biology and molecular basis of denitrification, Microbiol Mol. Biol. R., 61, 533–616, 1997.

Discussion Paper | Discussion Paper | Discussion Paper | Discussion Paper |

BGD

12, 13545–13591, 2015

Nitrogen cycling in deep-sea porewaters

S. D. Wankel et al.

Title Page

Abstract | Introduction

Conclusions | References

Tables | Figures

|◄ | ►|

◄ | ►

Back | Close

Full Screen / Esc

Printer-friendly Version

Interactive Discussion

Table 1. Modeled reaction nitrification and denitrificaiton rates in porewaters at North Pond. Sensitivity of rates to model prescribed values of $^{15}\varepsilon_{DNF}$ for transitional intervals are also shown.

				Modeled Reaction Rates											
				Nitrification (nmol cm^{-3} yr^{-1})						Denitrification (nmol cm^{-3} yr^{-1})					
				$^{15}\varepsilon_{DNF}=25$		$^{15}\varepsilon_{DNF}=15$		$^{15}\varepsilon_{DNF}=5$		$^{15}\varepsilon_{DNF}=25$		$^{15}\varepsilon_{DNF}=15$		$^{15}\varepsilon_{DNF}=5$	
Core ID	Depth mbsf	NO$_3$ µM	Model Zone	Rate	+/−	Rate	+/−	Rate	+/−	Rate	+/−	Rate	+/−	Rate	+/−
U1382B	0.9	34.4	Oxic	161.0	34.3	–	–	–	–	–	–	–	–	–	–
U1382B	3.3	34.7	Transitional	183.0	22.3	169.7	50.4	83.6	21.6	1.0	0.6	0.4	0.2	42.3	12.4
U1382B	6.1	35.1	Transitional	655.5	120.7	457.7	99.3	292.6	54.6	23.9	15.3	25.3	16.7	614.1	133.0
U1382B	7.6	35.3	Transitional	428.4	68.1	405.9	60.8	227.6	34.5	29.5	18.2	5.7	3.0	327.7	53.5
U1382B	11.7	36.1	Transitional	479.7	61.6	614.9	80.7	272.0	40.9	38.6	13.0	20.8	8.5	507.2	34.7
U1382B	18.0	36.5	Transitional	98.1	23.4	109.6	37.8	283.9	42.5	83.8	7.1	13.9	3.0	151.4	42.7
U1382B	27.9	36.1	Transitional	99.9	30.2	155.9	34.7	252.9	55.2	352.9	54.6	18.8	4.3	77.6	47.4
U1382B	32.1	35.5	Anoxic	–	–	–	–	–	–	130.5	7.9	–	–	–	–
U1382B	36.3	35.0	Anoxic	–	–	–	–	–	–	310.8	56.4	–	–	–	–
U1382B	41.6	34.7	Anoxic	–	–	–	–	–	–	7.7	1.4	–	–	–	–
U1382B	59.8	33.3	Anoxic	–	–	–	–	–	–	59.5	5.0	–	–	–	–
U1382B	67.7	32.5	Anoxic	–	–	–	–	–	–	199.8	35.3	–	–	–	–
U1382B	70.8	32.1	Transitional	870.6	144.9	460.0	84.5	558.7	156.3	578.5	60.7	147.3	71.7	238.1	70.5
U1382B	72.9	31.7	Transitional	304.0	44.7	266.6	68.4	376.6	101.8	515.8	79.0	35.6	13.6	169.8	51.5
U1382B	79.6	31.1	Oxic	182.0	39.9	–	–	–	–	–	–	–	–	–	–
U1382B	85.4	29.7	Oxic	221.2	26.0	–	–	–	–	–	–	–	–	–	–
U1382B	89.3	28.8	Oxic	–	–	–	–	–	–	–	–	–	–	–	–
U1383D	3.5	34.5	Oxic	29.0	5.3	–	–	–	–	–	–	–	–	–	–
U1383D	6.3	35.7	Oxic	100.4	31.8	–	–	–	–	–	–	–	–	–	–
U1383D	7.5	36.5	Oxic	221.1	78.0	–	–	–	–	–	–	–	–	–	–
U1383D	10.0	37.2	Transitional	271.6	50.5	148.0	27.5	236.2	61.7	1.4	0.7	2.9	1.0	158.0	100.0
U1383D	12.5	38.0	Transitional	304.1	33.9	321.9	33.9	330.4	56.5	7.6	5.1	12.3	6.3	187.8	55.9
U1383D	17.3	38.7	Transitional	235.6	60.4	261.7	54.1	268.0	55.5	3.6	2.0	18.2	8.4	317.8	50.8
U1383D	20.0	39.2	Transitional	526.2	188.8	402.3	95.9	439.8	157.1	14.8	13.0	15.7	9.3	667.2	260.8
U1383D	21.0	39.4	Transitional	177.1	83.3	420.5	198.0	554.9	70.5	29.0	3.3	131.8	59.1	576.7	88.1
U1383D	23.0	39.3	Transitional	514.8	114.8	385.7	100.4	762.5	79.2	14.6	6.0	88.6	38.8	877.3	233.6
U1383D	25.0	39.1	Transitional	240.1	60.9	101.3	35.6	509.9	108.1	22.2	4.1	85.1	13.2	364.3	70.7
U1383D	29.5	38.7	Transitional	71.1	23.5	95.8	35.7	214.1	65.6	3.3	0.7	22.0	4.8	96.0	32.7
U1383D	31.5	37.7	Transitional	16.2	4.4	28.6	7.9	57.2	17.1	0.3	0.1	2.0	0.7	18.0	6.9
U1383D	34.4	34.5	Transitional	78.1	32.1	26.7	7.4	23.5	8.7	0.7	0.3	1.1	0.5	3.4	1.9
U1383D	37.0	32.8	Transitional	286.4	19.0	281.7	61.7	530.9	153.2	19.3	10.6	103.5	32.6	246.5	65.9
U1383D	40.4	30.9	Transitional	–	–	–	–	–	–	–	–	–	–	–	–
U1384A	10.8	36.9	Transitional	45.0	9.0	62.5	9.6	75.2	21.8	0.1	0.0	2.4	2.3	31.8	24.2
U1384A	14.4	37.5	Transitional	105.8	27.9	117.6	55.5	256.9	110.2	1.3	1.1	1.5	1.5	100.0	55.2
U1384A	18.6	38.4	Transitional	24.9	6.8	26.4	10.9	104.8	78.6	0.2	0.2	0.3	0.2	60.6	47.6
U1384A	29.6	41.8	Transitional	65.2	8.7	49.7	12.9	78.6	58.4	0.2	0.1	0.1	0.0	58.2	42.7
U1384A	38.8	43.8	Anoxic	–	–	–	–	–	–	6.4	0.0	–	–	–	–
U1384A	44.1	43.9	Anoxic	–	–	–	–	–	–	23.9	3.0	–	–	–	–
U1384A	55.6	44.2	Transitional	20.1	9.2	23.6	9.9	11.3	3.4	0.1	0.0	0.2	0.1	6.5	1.9
U1384A	68.4	39.7	Transitional	40.9	16.2	36.1	23.8	30.5	9.9	0.1	0.1	0.8	0.7	18.7	7.9
U1384A	75.4	37.3	Oxic	13.1	2.6	–	–	–	–	–	–	–	–	–	–
U1384A	85.7	33.8	Oxic	–	–	–	–	–	–	–	–	–	–	–	–

Table 2. Denitrification isotope effects $^{15}\varepsilon_{DNF}$ and $^{18}\varepsilon{:}^{15}\varepsilon_{DNF}$ estimated from anoxic porewaters at North Pond.

Core ID	Depth mbsf	Denitrification Parameters	
		$^{15}\varepsilon_{DNF}$	$^{18}\varepsilon{:}^{15}\varepsilon_{DNF}$
U1382B	32.1	21.0 ± 0.3	0.99 ± 0.02
U1382B	36.3	21.9 ± 0.4	0.95 ± 0.02
U1382B	41.6	20.7 ± 0.1	0.84 ± 0.01
U1382B	59.8	18.8 ± 0.3	1.07 ± 0.02
U1382B	67.7	17.4 ± 0.4	1.11 ± 0.02
U1384A	38.8	*	*
U1384A	44.1	8.1 ± 0.2	1.08 ± 0.04

* changes in δ^{15}N and δ^{18}O were too small over this interval for resolving a reliable estimate of $^{15}\varepsilon$ or $^{18}\varepsilon{:}^{15}\varepsilon$.

Nitrogen cycling in deep-sea porewaters

S. D. Wankel et al.

Printer-friendly Version

Interactive Discussion
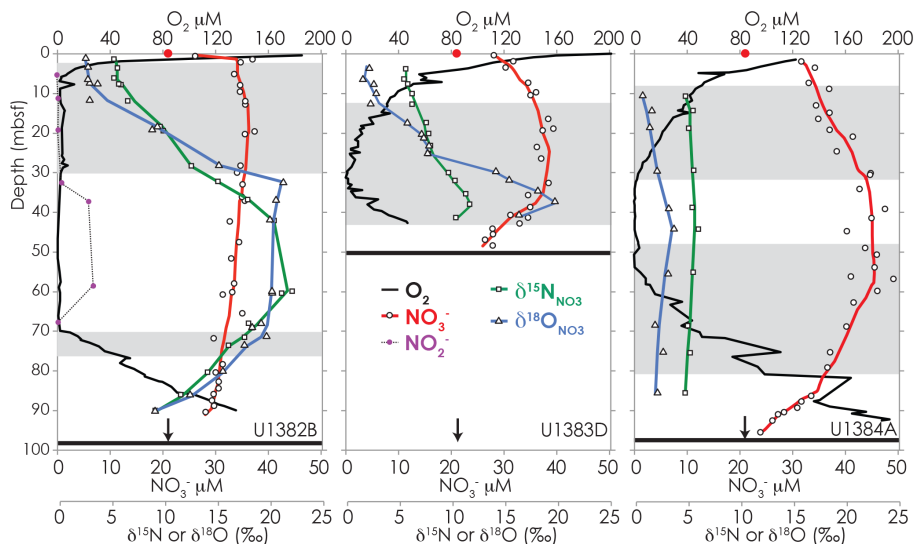
Figure 1. Depth profiles from IODP sites U1382B, U1383D and U1384A at North Pond of porewater concentrations of O_2 (from Orcutt et al., 2013) and NO_3^- as well as the N and O isotopic composition of NO_3^-. ($\delta^{15}N_{NO_3}$ and $\delta^{18}O_{NO_3}^-$). The red circle at the top of the profiles denotes the bottom seawater NO_3^- concentration of 21.6 μM (Ziebis et al., 2012). Horizontal black lines indicate depth of contact with ocean crust. Gray boxes indicate "transitional" zones in which a reaction–diffusion model is used to calculate co-occurring nitrification and denitrification (see text for details). Strong increases in $\delta^{15}N$ and $\delta^{18}O$ in U1382B coincide with depths having the lowest O_2 concentration and are indicative of the influence of denitrification. While the NO_3^- concentrations profiles of U1383D and U1384A appear similar, stark differences in the nitrate dual isotopic composition reflect the generally low level of microbial activity in U1384A.

Full Screen / Esc

Printer-friendly Version

Interactive Discussion
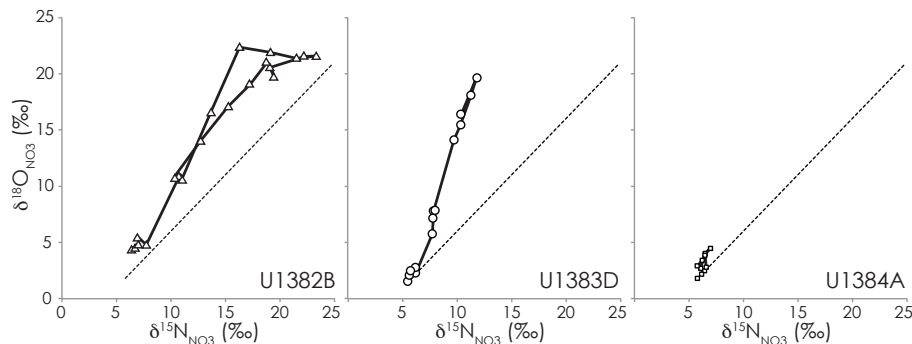
Figure 2. Dual isotope plot illustrating the relationship between $\delta^{15}N_{NO_3}$ and $\delta^{18}O_{NO_3}$ in North Pond porewaters. The diagonal line, rooted at a value for bottom seawater ($\delta^{15}N$ of +5.5 ‰ and $\delta^{18}O$ of +1.8 ‰), depicts a 1 : 1 slope representative of the expected change in $\delta^{15}N$ and $\delta^{18}O$ by the process of denitrification alone. Trends falling well above this 1 : 1 line, together with the concentration profiles reflect the combined role of nitrification in these porewaters.
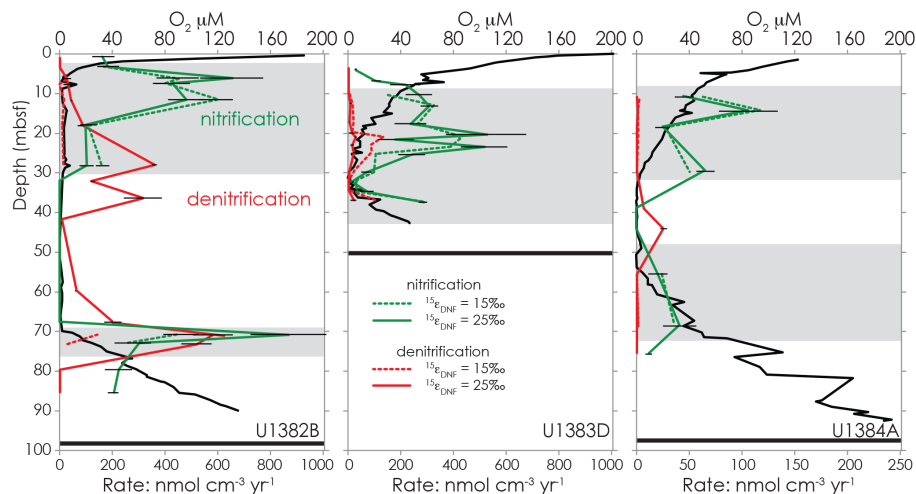
Figure 3. Model estimated rates of denitrification and nitrification ($nmol\,cm^{-3}\,yr^{-1}$) based on fitting of nitrate concentration and N and O isotopic composition. Estimates within transitional intervals are calculated using a value for $^{15}\varepsilon_{DNF}$ of either 15‰ (dashed) or 25‰ (solid). Error bars are shown for the $^{15}\varepsilon_{DNF} = 25$‰ only and indicate the standard error of 10 model runs (see text). Note the different scales for rates among the three profiles.
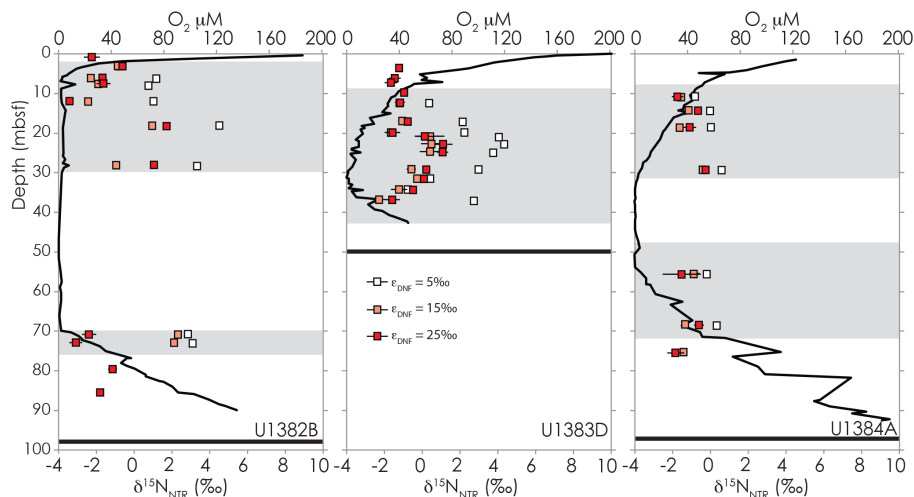
Figure 4. Model estimated values for the N isotopic composition of new nitrate produced by nitrification ($\delta^{15}N_{NTR}$) occurring within porewaters. Values are calculated for depths at which O_2 concentrations were $> 2\,\mu M$ (e.g., oxic and transitional intervals). Sensitivity of $\delta^{15}N_{NTR}$ to prescribed values of the isotope effect for denitrification ($^{15}\varepsilon_{DNF}$) in transitional intervals, where both nitrification and denitrification can co-occur, is also indicated.

Full Screen / Esc

Printer-friendly Version

Interactive Discussion

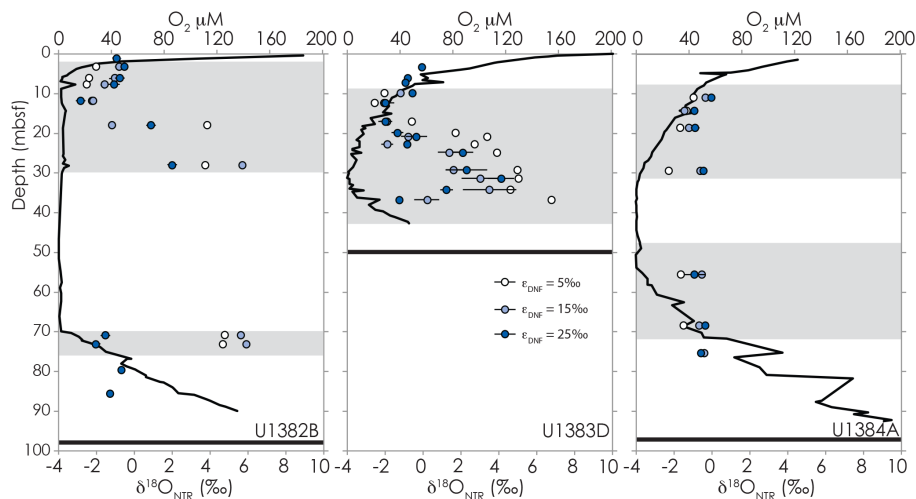**Figure 5.** Model estimated values for the O isotopic composition of new nitrate produced by nitrification ($\delta^{18}O_{NTR}$) occurring within porewaters. Values are calculated for depths at which O_2 concentrations were > 2 µM (e.g., oxic and transitional intervals). Sensitivity of $\delta^{18}O_{NTR}$ to prescribed values of the isotope effect for denitrification ($^{15}\varepsilon_{DNF}$) in transitional intervals, where both nitrification and denitrification can co-occur, is also indicated.